

AFCRL-TR-75-0528  
PHYSICAL SCIENCES RESEARCH PAPERS, NO. 645

10  
B.S.



ADA020292

## High-Energy Laser — Target Interactions

ROBERT J. PAPA  
RICHARD L. TAYLOR

6 October 1975

Approved for public release; distribution unlimited.

D D C  
RECEIVED  
FEB 9 1976  
A

MICROWAVE PHYSICS LABORATORY PROJECT 2153  
AIR FORCE CAMBRIDGE RESEARCH LABORATORIES  
HANSCOM AFB, MASSACHUSETTS 01731

AIR FORCE SYSTEMS COMMAND, USAF



Qualified requestors may obtain additional copies from the Defense Documentation Center. All others should apply to the National Technical Information Service.

Unclassified SECURITY CLASSIFICATION OF THIS PAGE (When Data Entered)		READ INSTRUCTIONS BEFORE COMPLETING FORM	
REPORT DOCUMENTATION PAGE		RECIPIENT'S CATALOG NUMBER	
1. REPORT NUMBER <b>AFCRL-TR-75-0528</b>	2. GOVT ACCESSION NO. <b>AFCRL-PSRP-645</b>	3. TYPE OF REPORT & PERIOD COVERED <b>Scientific, Interim.</b>	
4. TITLE (and Subtitle) <b>HIGH-ENERGY LASER - TARGET INTERACTIONS</b>	5. PERFORMING ORG. REPORT NUMBER <b>PSRP No. 645</b>		
7. AUTHOR(s) <b>Robert J. Papa Richard L. Taylor</b>	8. CONTRACT OR GRANT NUMBER(s)		
9. PERFORMING ORGANIZATION NAME AND ADDRESS <b>Air Force Cambridge Research Laboratories (LZR) Hanscom AFB Massachusetts 01731</b>		10. PROGRAM ELEMENT, PROJECT, TASK AREA & WORK UNIT NUMBERS <b>215303ba 16 AF-2153 681305, 61192F</b>	
11. CONTROLLING OFFICE NAME AND ADDRESS <b>Air Force Cambridge Research Laboratories (LZR) Hanscom AFB Massachusetts 01731</b>		12. REPORT DATE <b>October 1975</b>	
14. MONITORING AGENCY NAME & ADDRESS (if different from Controlling Office) <b>(11) 6 Oct 75 (12) 66 p.</b>		13. NUMBER OF PAGES <b>66</b>	
		15. SECURITY CLASS. (of this report) <b>Unclassified</b>	
16. DISTRIBUTION STATEMENT (of this Report) <b>Approved for public release; distribution unlimited.</b>		15a. DECLASSIFICATION/DOWNGRADING SCHEDULE	
9. <b>Physical Sciences Research Papers</b>			
17. DISTRIBUTION STATEMENT (of the abstract entered in Block 20, if different from Report)			
18. SUPPLEMENTARY NOTES			
19. KEY WORDS (Continue on reverse side if necessary and identify by block number) <b>High-energy laser interactions Ignition of laser absorption waves</b>			
20. ABSTRACT (Continue on reverse side if necessary and identify by block number) <b>A general model of high-energy laser interactions with solid surfaces is presented. Fluid transport equations are used to describe the heating and vaporization of a solid surface irradiated by intense laser energy. The vaporized target material diffuses into an ambient gas. Both the target vapor and ambient gas can ionize. Separate transport equations are used for the ambient gas, the gas of atoms in an excited state, the electrons, the target vapor, the ionized ambient gas, and the ionized target vapor. Among the over 30 physical processes included in the model are: laser wave absorption, electron and ion</b>			

DD FORM 1473 EDITION OF 1 NOV 65 IS OBSOLETE

Unclassified  
SECURITY CLASSIFICATION OF THIS PAGE (When Data Entered)

011 800




CONTINUED

Unclassified

SECURITY CLASSIFICATION OF THIS PAGE(When Data Entered)

20. Abstract (continued)

gas heating, diffusion of each species, excitation collisions, recombination, radiation transport, photoionization, shock formation, cascade ionization, thermionic emission, neutral impact ionization and energy, and momentum transfer among all fluid species. A computer program has been developed to numerically integrate these transport equations. The ignition and propagation of laser-supported absorption waves (LAWS) are studied as a function of incident power level. Graphs are presented of the temperature and density profiles of each species at various instants in time as a function of the incident laser power level.



Unclassified

SECURITY CLASSIFICATION OF THIS PAGE(When Data Entered)

## Contents

1. INTRODUCTION	7
2. MULTIFLUID TRANSPORT EQUATIONS	15
3. CONCLUSIONS	41
REFERENCES	65

## Illustrations

1. Particle Density vs Normalized Distance (E = 0 MV/m; Time = $0.257 \times 10^{-6}$ sec)	46
2. Temperature ( $^{\circ}$ K) vs Normalized Distance (E = 0 MV/m; Time = $0.257 \times 10^{-6}$ sec)	46
3. Particle Density vs Normalized Distance (E = 6 MV/m; Time = $0.618 \times 10^{-6}$ sec)	47
4. Temperature ( $^{\circ}$ K) vs Normalized Distance (E = 6 MV/m; Time = $0.618 \times 10^{-6}$ sec)	47
5. Particle Density vs Normalized Distance (E = 6 MV/m; Time = $1.411 \times 10^{-6}$ sec)	48
6. Temperature ( $^{\circ}$ K) vs Normalized Distance (E = 6 MV/m; Time = $1.411 \times 10^{-6}$ sec)	48
7. Particle Density vs Normalized Distance (E = 20 MV/m; Time = $0.048 \times 10^{-6}$ sec)	49

## Illustrations

8.	Temperature ( $^{\circ}\text{K}$ ) vs Normalized Distance ( $E = 20 \text{ MV/m}$ ; Time = $0.048 \times 10^{-6} \text{ sec}$ )	49
9.	Particle Density vs Normalized Distance ( $E = 20 \text{ MV/m}$ ; Time = $0.103 \times 10^{-6} \text{ sec}$ )	50
10.	Temperature ( $^{\circ}\text{K}$ ) vs Normalized Distance ( $E = 20 \text{ MV/m}$ ; Time = $0.103 \times 10^{-6} \text{ sec}$ )	50
11.	Particle Density vs Normalized Distance ( $E = 6 \text{ MV/m}$ ; Time = $0.248 \times 10^{-6} \text{ sec}$ )	51
12.	Temperature ( $^{\circ}\text{K}$ ) vs Normalized Distance ( $E = 6 \text{ MV/m}$ ; Time = $0.248 \times 10^{-6} \text{ sec}$ )	51
13.	Particle Density vs Normalized Distance ( $E = 6 \text{ MV/m}$ ; Time = $0.549 \times 10^{-6} \text{ sec}$ )	52
14.	Temperature ( $^{\circ}\text{K}$ ) vs Normalized Distance ( $E = 6 \text{ MV/m}$ ; Time = $0.549 \times 10^{-6} \text{ sec}$ )	52
15.	Particle Density vs Normalized Distance ( $E = 6 \text{ MV/m}$ ; Time = $0.832 \times 10^{-6} \text{ sec}$ )	53
16.	Temperature ( $^{\circ}\text{K}$ ) vs Normalized Distance ( $E = 6 \text{ MV/m}$ ; Time = $0.832 \times 10^{-6} \text{ sec}$ )	53
17.	Particle Density vs Normalized Distance ( $E = 6 \text{ MV/m}$ ; Time = $1.457 \times 10^{-6} \text{ sec}$ )	54
18.	Temperature ( $^{\circ}\text{K}$ ) vs Normalized Distance ( $E = 6 \text{ MV/m}$ ; Time = $1.457 \times 10^{-6} \text{ sec}$ )	54
19.	Particle Density vs Normalized Distance ( $E = 20 \text{ MV/m}$ ; Time = $0.046 \times 10^{-6} \text{ sec}$ )	55
20.	Temperature ( $^{\circ}\text{K}$ ) vs Normalized Distance ( $E = 20 \text{ MV/m}$ ; Time = $0.046 \times 10^{-6} \text{ sec}$ )	55
21.	Particle Density vs Normalized Distance ( $E = 20 \text{ MV/m}$ ; Time = $0.061 \times 10^{-6} \text{ sec}$ )	56
22.	Temperature ( $^{\circ}\text{K}$ ) vs Normalized Distance ( $E = 20 \text{ MV/m}$ ; Time = $0.061 \times 10^{-6} \text{ sec}$ )	56
23.	Particle Density vs Normalized Distance ( $E = 20 \text{ MV/m}$ ; Time = $0.074 \times 10^{-6} \text{ sec}$ )	57
24.	Temperature ( $^{\circ}\text{K}$ ) vs Normalized Distance ( $E = 20 \text{ MV/m}$ ; Time = $0.074 \times 10^{-6} \text{ sec}$ )	57
25.	Particle Density vs Normalized Distance ( $E = 20 \text{ MV/m}$ ; Time = $0.046 \times 10^{-6} \text{ sec}$ ; uncoupled diffusion)	58
26.	Temperature ( $^{\circ}\text{K}$ ) vs Normalized Distance ( $E = 20 \text{ MV/m}$ ; Time = $0.046 \times 10^{-6} \text{ sec}$ ; uncoupled diffusion)	58
27.	Particle Density vs Normalized Distance ( $E = 30 \text{ MV/m}$ ; Time = $0.074 \times 10^{-6} \text{ sec}$ ; uncoupled diffusion)	59
28.	Temperature ( $^{\circ}\text{K}$ ) vs Normalized Distance ( $E = 20 \text{ MV/m}$ ; Time = $0.074 \times 10^{-6} \text{ sec}$ ; uncoupled diffusion)	59
29.	Particle Density vs Normalized Distance ( $E = 20 \text{ MV/m}$ ; Time = $0.079 \times 10^{-6} \text{ sec}$ )	60

## Illustrations

30.	Temperature ( $^{\circ}\text{K}$ ) vs Normalized Distance ( $E = 20 \text{ MV/m}$ ; Time = $0.079 \times 10^{-6} \text{ sec}$ )	60
31.	Particle Density vs Normalized Distance ( $E = 20 \text{ MV/m}$ ; Time = $0.080 \times 10^{-6} \text{ sec}$ )	61
32.	Temperature ( $^{\circ}\text{K}$ ) vs Normalized Distance ( $E = 20 \text{ MV/m}$ ; Time = $0.080 \times 10^{-6} \text{ sec}$ )	61
33.	Particle Density vs Normalized Distance ( $E = 20 \text{ MV/m}$ ; Time = $0.093 \times 10^{-6} \text{ sec}$ )	62
34.	Temperature ( $^{\circ}\text{K}$ ) vs Normalized Distance ( $E = 20 \text{ MV/m}$ ; Time = $0.093 \times 10^{-6} \text{ sec}$ )	62
35.	Particle Density vs Normalized Distance ( $E = 20 \text{ MV/m}$ ; Time = $0.100 \times 10^{-6} \text{ sec}$ )	63
36.	Temperature ( $^{\circ}\text{K}$ ) vs Normalized Distance ( $E = 20 \text{ MV/m}$ ; Time = $0.100 \times 10^{-6} \text{ sec}$ )	63
37.	Particle Density vs Normalized Distance ( $E = 20 \text{ MV/m}$ ; Time = $0.102 \times 10^{-6} \text{ sec}$ )	64
38.	Temperature ( $^{\circ}\text{K}$ ) vs Normalized Distance ( $E = 20 \text{ MV/m}$ ; Time = $0.102 \times 10^{-6} \text{ sec}$ )	64

# High-Energy Laser—Target Interactions

## 1. INTRODUCTION

The interaction of high-energy laser radiation with a solid surface can produce many physical processes. These processes include the following: absorption of laser radiation by a solid target, thermal conduction into target, vaporization of target material, diffusion of target material into an ambient gas, thermionic emission from heated target surface, cascade ionization of target vapor and ambient gas atoms, heating of electrons and ions by inverse bremsstrahlung, excitation and de-excitation collisions, energy and momentum transfer among all species, neutral impact ionization, photoionization, radiation transport, shock formation, attenuation of laser radiation by plasma, diffusion of each species, electrical coupling between the electrons and each ion species, recombination, electron impact ionization from excited states, and so forth.

---

(Received for publication 3 October 1975)



Previous works in this field (Ready,<sup>1</sup> DeMichellis,<sup>2,3</sup> Nielsen,<sup>4</sup> Nielsen and Canavan,<sup>5</sup> Harmon<sup>6</sup>) have included some of these mechanisms, but not all in a self-consistent theory. Most of the previous studies have treated the problem using a one-, or at most, two-fluid model with separate electron and heavy-particle temperatures.<sup>7,8</sup> In these treatments, the ion temperature is assumed to be equal to the heavy-particle temperature. However, especially in the immediate vicinity of the target surface, these assumptions may not be entirely valid, since the expanding target vapor is much hotter than the ambient gas. Also, since the rate of diffusion of the ions is coupled to that of the electrons, the cooling by expansion for the ions will be different from that for the neutral species. Finally, relaxation times between species can greatly increase so that the time for energy equilibration may become quite large. Indeed, it has been shown that by assuming an initial electron density of about  $10^{16}$  part/cm<sup>3</sup> over a distance of several laser wavelengths (10.6  $\mu$ m), for incident laser power levels greater than  $3 \times 10^8$  watts/cm<sup>2</sup> in xenon, the ion temperature can be different than the heavy particle temperature.<sup>9</sup>

P. D. Thomas<sup>10</sup> has performed computer solutions for the ignition of laser absorption waves (LAW's) based on a uniform vaporization model that takes into account gas dynamics and radiative transport in the interaction region over the surface, and for heat conduction within the target. Thomas<sup>10</sup> has compared his

1. Ready, J. F. (1971) Effects of High-Power Laser Radiation, Academic Press.
2. DeMichellis, C. (1969) IEEE J. Quant. Electronics QE-5:188.
3. DeMichellis, C. (1970) IEEE J. Quant. Electronics QE-6:630.
4. Nielsen, P. E. (1974) Breakdown and laser absorption waves, Jour. Defense Research, Series B, December.
5. Nielsen, P. E. and Canavan, G. H. (1974) Theory of laser target interaction, Jour. Defense Research, Series B, December.
6. Harmon, N. F. (1974) Proceedings of the 1973 DoD Laser Effects/Hardening Conference (U), Vol. V, Laser supported absorption waves, Mitre Corp. Rpt M73-115.
7. Edwards, A., Ferriter, N. M., Fleck, J. A., and Winslow, A. M. (1974) A theoretical description of pulsed laser-target interaction in an air environment, published in Proceedings of the 1973 DoD Laser Effects/Hardening Conference (U), Vol. V (see ref. 6, p. 115).
8. Stamm, M. F. and Nielsen, P. E. (1974) Nonequilibrium effects in shock- and transport-induced LAW formation, published in Proceedings of the 1973 DoD Laser Effects/Hardening Conference (U), Vol. V (see ref. 6, p. 141).
9. Papa, R. J. (1974) Propagation of High-Power Laser Radiation in Partially Ionized Gases, AFRL-TR-74-0532.
10. Thomas, P. D. (1973) Laser-Absorption Wave Initiation in Air Over Vaporizing Targets (see ref. 6, p. 69).

calculations with the experimental results of Mathematical Sciences Northwest<sup>11</sup> and Battelle Memorial Institute.<sup>12</sup> Thomas concluded that a uniform vaporization model is probably valid at 10.6- $\mu$ m radiation for intensities of the order of a few times  $10^6$  watts/cm<sup>2</sup> or less, but the physics of the interaction is different above this intensity.

Musal<sup>13</sup> has noted that in the laser intensity range  $3 \times 10^7$  to  $3 \times 10^8$  watts/cm<sup>2</sup>, laser-supported absorption waves are ignited in times much shorter than that required to produce uniform surface vaporization. Musal has presented an analytic model of the field-emission/cascade-ionization buildup of the plasma over a small protrusion on the laser-irradiated target. Musal has concluded that the prompt initiation of laser-supported absorption waves at metallic surfaces at incident laser-beam intensities above  $5 \times 10^7$  watts/cm<sup>2</sup> are probably caused by cascade air breakdown initiated from localized plasmas generated in the ambient atmosphere by impact ionization from electrons field-emitted from surface protrusions.

Walters<sup>14</sup> has listed the following mechanisms for LAW ignition:

- (1) Uniform target vaporization
- (2) Oxide vapor absorption
- (3) Chemical reaction
- (4) Thermionic emission
- (5) Planar reflection-enhanced fields
- (6) Local target heating
- (7) Contaminant and gas desorption
- (8) Field emission
- (9) Shock heating of the air
- (10) Nonequilibrium ionization of the vapor
- (11) Defect enhanced fields

Using photographic, photometric, spectroscopic, electronic, and surface diagnostics, Walters<sup>14</sup> has assessed the role of the various LAW ignition mechanisms. He has concluded that thermionic emission and local target heating play a major role in the LAW ignition process.

11. Klosterman, E.L., Byron, S.R., and Newton, J.F. (1973) Laser Supported Combustion Waves Study Report No. 73-101-3, Mathematical Sciences Northwest, Inc., Seattle, Wash.
12. Walters, C.T. (1972) Review of Experiments at Battelle presented at the Workshop on Laser-Induced Combustion Waves, Seattle, Wash., 5-6 December 1972.
13. Musal, H.M. (1973) Prompt Initiation of Laser-Supported Absorption Waves in Air Via Field-Emission from Target Surfaces (see ref. 6, p. 157).
14. Walters, C.T. (1973) Experimental Studies of LSD Wave Initiation on Aluminum Targets (see ref. 6, p. 178).

In the present paper, mechanisms (1), (3), (4), (6), (8), (9), and (10) are included in a consistent fashion. Also, the effect of the ionized target vapor on the electron diffusion process is properly treated. Cohen et al.<sup>15</sup> have presented a method of analysis by which the electron cascade equations are coupled to the fluid mechanics conservation equations for the purpose of investigating the effect of a shock-induced flow field on breakdown. The laser plasma interaction is treated by an idealized single fluid model which includes unequal electron and heavy particle temperatures and a two-stage ionization model. A similar model has been used by Stamm and Nielsen.<sup>8</sup> However, the transport equations presented in references 8, 10, and 15 are such that some of the nonlinear convective derivative terms are neglected. Also, in the equations for the time rate of change of energy density, some of the terms representing the time rate of change of the fluid energy due to its convective motion are neglected. At high laser intensities, these terms may not be negligible.

Part of the purpose of the present report is to relax some of the assumptions that were made in references 1, 7, 8, 10, 13, and 15, in order to investigate their range of validity. For example, it may not always be appropriate to write down the continuity and energy equations in a single Lagrangian frame for all species, because this implies that the convective velocities of electrons, ions, and neutrals are all equal. Also, the electron diffusion coefficients, which are normally derived in an Eulerian (fixed frame), will differ in a Lagrangian frame. In addition, since the laser flux levels can reach quite high values, the nonlinear convective derivative terms in the momentum transfer equation for the electrons should not be neglected a priori. However, it can be shown that for 10.6- $\mu\text{m}$  flux levels up to  $5 \times 10^{11}$  watts/cm<sup>2</sup>, the nonlinear convective derivative terms in the electron gas can indeed be neglected (see Papa,<sup>9</sup> p. 54). Finally since the target ion density may become quite large in the vicinity of the target, the effect of the presence of two distinct ion species (target and ambient gas) on the electron diffusion coefficient should be investigated. The fluid transport equations, written in an Eulerian frame with no terms omitted, are given in Holt and Haskell,<sup>10</sup> pp. 156 to 166. These general equations are the ones used in this report.

The present report includes the following physical mechanisms describing high-energy laser-target interactions:

- (1) Laser wave absorption in a plasma and in the target;

---

15. Cohen, H.D., Su, F.Y., and Boni, A.A. (1973) A Simple Nonequilibrium Model for a Shock-Heated Monatomic Gas Irradiated by an Intense Laser Beam (see ref. 6, p. 239).

16. Holt, E.H. and Haskell, R.E. (1965) Foundations of Plasma Dynamics, Macmillan.

- (2) Electron and ion gas heating by inverse bremsstrahlung due to absorption of laser wave energy;
- (3) Electron diffusion coupled with the diffusion of the ambient gas ions and the target vapor ions;
- (4) Excitation of one energy level by electron impact on a neutral atom;
- (5) De-excitation of energy level by radiation;
- (6) Diffusion of resonant radiation and subsequent excitation of neutrals by resonant radiation absorption;
- (7) Electron impact ionization from ground state;
- (8) Electron impact ionization from excited level;
- (9) Diffusion of neutral-state atoms and excited-state atoms due to temperature and density gradients;
- (10) Recombination:
  - (a) radiative,
  - (b) electron-electron-ion,
  - (c) transitional;
- (11) Momentum transfer from laser wave to electron gas due to inhomogeneities in dielectric coefficient (nonlinear forces discussed by Hora<sup>17</sup>);
- (12) Thermal conduction in electron gas, ion gas, neutral gas, gas of excited atoms and target vapor;
- (13) Bremsstrahlung loss by electrons colliding with ions;
- (14) Radiative recombination cooling of electron gas;
- (15) Energy transfer by collisions between electrons and ions;
- (16) Energy transfer by collisions between electrons and neutrals;
- (17) Energy transfer by collisions between ions and neutrals;
- (18) Nonlinear convective derivative terms are retained in the momentum transfer equations.
- (19) Heating of the ions due to dynamic polarization of the plasma (Vinogradov and Pustovalov<sup>18</sup>);
- (20) Arbitrary laser frequency (so long as  $h\nu_L \ll E_{\text{excited}}$ , where  $E_{\text{excited}}$  = energy of excited state,  $h$  = Planck's constant and  $\nu_L$  = laser frequency, so that classical physics applies);
- (21) Arbitrary pulse length, pulse shape, and pulse repetition frequency;
- (22) Shock formation mechanisms;
- (23) Photo-ionization due to continuum radiation absorption from the ground state or from an excited state;

17. Hora, H. (1969) Phys. Fluids 12:182.

18. Vinogradov, A. V. and Pustovalov, V. V. (1972) Soviet Jour. Quant. Electronics 2:91.

- (24) Neutral-neutral impact ionization;
- (25) Absorption of laser energy into a target and thermal conduction into the target;
- (26) Vaporization of target material, with diffusion and ionization of target material into an ambient gas;
- (27) Thermionic emission from target surface;
- (28) Effect of target ions on electron ambipolar diffusion coefficient;
- (29) Energy and momentum exchange between target vapor and ambient gas particles;
- (30) Energy and momentum exchange between target vapor and electrons;
- (31) Ionization of target vapor by electron impact;
- (32) Ionization of target vapor by neutral-neutral impact.

In a previous report,<sup>9</sup> it was explained how multi-fluid transport equations can be used to describe the physical mechanisms (1) through (24). Mechanism (25), absorption of laser energy into a target, and thermal conduction into the target, are described in this present report by solving the one-dimensional heat-flow equation. The absorptivity and reflectivity of the target are functions of the incident laser-power level. In Fig. 3.26, p. 116 of reference 1, the reflectivity of various materials is plotted as a function of laser-power level for a Q-switched Nd-glass laser. In the present report, it is assumed that the reflectivity of a target has the same behavior under irradiation at 10.6  $\mu\text{m}$  wavelength. The solution to the heat-conduction equation for an arbitrary laser-pulse shape is given by Eq. (3.9), p. 73 of reference 1:

$$T_T(x, t) = \frac{\kappa^{1/2}}{K\sqrt{\pi}} \int_0^t d\tau \frac{F(t-\tau)}{\tau^{1/2}} \exp(-x^2/(4K\tau)) \quad (1)$$

where

- $T_T$  = temperature of target;
- $x$  = spatial position, with  $x = 0$  taken as target surface;
- $t$  = elapsed time;
- $\kappa$  = thermal diffusivity;
- $K$  = thermal conductivity;
- $F$  = absorbed laser flux as a function of time.

The target is assumed to vaporize according to a model proposed by Anisimov.<sup>19</sup> The surface temperature of the target is obtained by equating the absorbed laser energy density to the surface temperature rise times the specific heat plus the specific heat of vaporization:

$$F = \nu_{ss} \rho [C_p T' + L] \quad (2)$$

where

$\nu_{ss}$  = velocity of retreating target surface,

$\rho$  = target density,

$C_p$  = heat capacity per unit mass,

$T'$  = maximum target surface temperature,

$L$  = specific heat of vaporization per unit mass.

If  $N_T(z = L)$  is the density of target vapor atoms at the target surface, then

$$\nu_{ss} = h_a [1/N_T(L)] \frac{dN_T(L)}{dt} \quad (3)$$

where  $h_a$  = thickness of an atomic layer in target material.

The continuity equation for the target vapor just at the target surface is given by

$$\frac{dN_T}{dt} = N_T \nu_o \exp(-LM/N_o kT') \quad (4)$$

where

$\nu_o$  = Debye frequency,

$M$  = atomic weight of target material,

$N_o$  = Avogadro's number,

$k$  = Boltzmann's constant.

Combining equations (2), (3), and (4) gives an implicit equation for the maximum target surface temperature  $T'$ :

$$F = h_a \nu_o \rho [C_p T' + L] \exp(-LM/N_o kT') \quad (5)$$

19. Anisimov, S.I. (1967) Soviet Phys. Tech. Phys. 11:945.

The fluid transport equations governing the target vapor density and temperature are similar to the transport equations for the other species, such as ambient-gas atoms, excited-state atoms, electrons, ambient-gas ions, and target vapor ions (Holt and Haskell,<sup>16</sup> pp. 156-166).

A very general computer program has been developed to solve this complicated set of nonlinear, partial differential equations. The program gives the laser intensity at any point from  $x = -\infty$  up to the target surface  $x = L$ . The attenuation of the laser beam due to any ionized particles generated by the interactions is accounted for by representing the laser electric-field intensity through the WKB approximation. Equation (1) is solved numerically for the target surface temperature,  $T_T(x = L)$ . Then Eq. (2) is solved for  $T'$  using the Newton-Raphson method (Stark,<sup>20</sup> p. 85); but  $T_T(x = L)$  cannot exceed  $T'$ . Equation (4) is solved for  $N_T$ , the target-vapor density, just at the target surface. The fluid transport equations for the target-vapor density and temperature, ambient-gas density and temperature, excited-state atom density, electron density and temperature, ambient-gas ion density, target-vapor ion density, and ion temperature are coupled to Maxwell's equations which govern the laser wave-propagation characteristics.

As explained in a previous report,<sup>9</sup> the plasma transport equations are of the telegraph type (Holt and Haskell,<sup>16</sup> p. 186). The coupled, partial differential equations are converted into a system of difference equations. A partially implicit, partially explicit (PI-PE) scheme for numerically integrating these transport equations is used for purposes of maintaining numerical stability, even when a large time step is selected. The PI-PE technique for integrating transport equations in time is discussed by Richtmyer and Morton.<sup>21</sup> The resulting system of difference equations for the particle densities, fluxes, and temperatures is solved at each time step by inverting a band-structured matrix. An efficient computer algorithm has been developed for inverting such band-structured matrices.

At each time step, the electromagnetic-field distribution and the transmission coefficient are calculated by using the WKB method to solve the wave equation. Also, if the percent change of all species is less than a certain tolerance from one time step to the next, the time step is increased. If the percent change of any one species is greater than a certain tolerance from one time step to the next, the time step is decreased. Finally, if the percent change of density or temperature of any one species is less than a certain tolerance for ten consecutive time steps, that particular species is "frozen out" for ninety consecutive time steps.

The various species that are involved in the high-energy laser - target interactions include: electrons, target-vapor ions, ambient-gas ions, ambient gas atoms

20. Stark, P.A. (1970) Introduction to Numerical Methods, Macmillan.

21. Richtmyer, R.D. and Morton, K.W. (1967) Difference Methods for Initial Value Problems, Interscience.

excited-state atoms, and target vapor. Thus, there are six sets of coupled fluid equations. For a given set of initial conditions, laser-pulse shape, pulse height, pulse length and target conditions, graphs are presented of the particle densities and temperatures as a function of position at different instants in time. In this particular report the ambient gas is chosen to be xenon, the laser wavelength is  $10.6 \mu\text{m}$ , and the target is aluminum.

## 2. MULTIFLUID TRANSPORT EQUATIONS

In reference 9, the multifluid transport equations were given for a high-intensity laser wave propagating through a partially ionized plasma. These equations were presented after making 27 self-consistent assumptions. In the present report, target heating due to laser absorption, target vaporization, diffusion of target vapor and ionization of target vapor are described, so that ignition and propagation of LAW's may be systematically investigated. Thus, in addition to the assumptions listed in the report by Papa,<sup>9</sup> several additional assumptions are added in order to include the target interactions.

A list of all these assumptions follows:

- (1) It is assumed that there are no variations of the plasma parameters in the y or z direction, only in the x direction (direction of laser wave propagation). The variation of the electric field intensity is also neglected in the y and z directions. These assumptions are reasonable, provided the diameter of the laser beam is much larger than any characteristic lengths in the plasma (such as Debye length, diffusion length, and scale lengths for temperature and density gradients).
- (2) The heat flux tensor is assumed to be isotropic for thermal conduction in the electron gas, ion gas, and neutral gas.
- (3) There is only one excitation potential  $E_{\text{ex}}$  of the neutral gas.
- (4) The electric field vector  $E_y$  is transverse to the direction of wave propagation. The incident laser wave is a plane wave.
- (5) There are no inelastic collisions of the second kind; only electron impact and absorption of resonant radiation can excite the neutral particles to the energy level  $E_{\text{ex}}$ .
- (6) There is no multiphoton absorption.
- (7) The electron and ion energy changes are assumed to occur continuously, so that the electron energy gain and loss terms are treated according to the laws of classical physics. This assumes the laser photon energy is 1 eV or less ( $\text{CO}_2$  laser).
- (8) It is assumed that at  $t = 0$  the electron-density profile  $N_e(x, t = 0)$ , the ion-density profile  $N_i(x, t = 0)$ , and the neutral-gas-density profile  $N_N(x, t = 0)$  are



known. Also, the electron temperature  $T_e(x, t = 0)$ , ion temperature  $T_i(x, t = 0)$  and neutral-gas temperature  $T_N$  are assumed to be known at  $t = 0$ . These initial electrons and ions are not due to the prebreakdown ionization observed by Papoular,<sup>22</sup> since LAW's may be ignited from targets at laser fluxes lower than that required to initiate breakdown in clean gases without a target. These initial conditions may have been the result of several different types of phenomena, such as the direct emission of particles from the target surface due to either photoelectric effect, thermionic emission, multiphoton absorption, or the tunneling effect. Keldysh<sup>23</sup> has shown that a frequency-dependent tunneling mechanism becomes equivalent to multiphoton ionization in the high-frequency limit.

(9) The possibility of shock generation occurring in the emerging target vapor will be neglected; shocks can form only in the ambient gas.

(10) Each atom is assumed to be capable of being only singly ionized so that multiple ionization effects are neglected. Only the following ionization mechanisms are considered:

(a) neutral-neutral gas atom impact ionization



(b) neutral-neutral target vapor atom impact ionization



(c) neutral-target vapor atom—neutral-gas atom impact ionization



(d) electron-neutral gas atom impact ionization



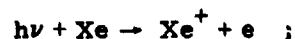
(e) electron-neutral target vapor atom impact ionization



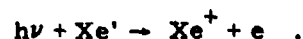
22. Papoular, R. (1972) The initial stages of laser induced gas breakdown, article in Laser Interaction and Related Plasma Phenomena, Vol. 2, Proc. of the Second Workshop held at RPI, Hartford Graduate Center, edited by H.J. Schwarz and H. Hora, Plenum Press.

23. Keldysh, L. V. (1965) Soviet Physics JETP 21:1135.

- (f) photo-ionization of the neutral-gas atoms by radiation from free-free transitions



- (g) photoionization of excited-state atoms by radiation from free-free transitions



(11) Inelastic ion-neutral collisions are neglected, which implies that charge-transfer reactions and ion-neutral impact ionizations are neglected.

(12) The Thomson cross section for scattering of laser radiation by free electrons is assumed to be negligible.

(13) Light scattering from electron-density fluctuations as discussed by Ramsden<sup>24</sup> is negligible.

(14) The heating of the electrons by stimulated Compton scattering, as discussed by Vinogradov and Pustovalov,<sup>18</sup> is negligible. However, the heating of the ion gas, due to the dynamic polarization of the plasma at the frequency of the scattered photons, is included.

(15) The radiation at frequency  $\nu_{\text{ex}} = E_{\text{ex}}/h$  is assumed to have a very small mean-free path in the plasma. Thus, the plasma is optically thick at this frequency and only the wings of the resonant radiation line can diffuse. This implies that the bound-bound absorption cross section is large. The diffusion of the resonant radiation is treated in the manner discussed by Myshenkov and Raizer.<sup>25</sup>

(16) The electron-distribution function, the ion-distribution function, the neutral ambient-gas atom distribution function, and the target-vapor atom distribution function are all assumed to be close to Maxwellian, so that one may define an effective electron temperature  $T_e$ , an effective ion temperature  $T_i$ , an effective neutral gas temperature  $T_N$ , and a target vapor temperature  $T_T$ . Thus, the Maxwellianization times for each species are assumed to be shorter than any time scales for temperature or density changes.

(17) The neutral gas particles in the excited state  $E_{\text{ex}}$  are assumed to have the same translational temperature  $T_N$  as the atoms in the ground state.

(18) The electron pressure tensor, the ion pressure tensor, the neutral gas pressure tensor, and the target vapor-pressure tensor are all assumed to be isotropic.

24. Ramsden, S.A. (1968) Physics of Hot Plasmas, Scottish Universities Summer School, Plenum Press.

25. Myshenkov, V.I. and Raizer, Yu. P. (1972) Soviet Phys. JETP 34:1001.

- (19) There is no dc magnetic field present.
- (20) There is no effect on the plasma processes due to metastable states.
- (21) The plasma is assumed to remain nonrelativistic, so that the effect of the ac magnetic field is negligible compared with the ac electric field (except insofar as the ac magnetic field contributes to the nonlinear force discussed by Hora<sup>17</sup>).
- (22) The wave period  $T = 2\pi/\omega$  of the laser radiation is much shorter than the time scale for electron density and temperature changes, so that the electric field  $E_y$  remains monochromatic in the time-varying plasma (Papa<sup>26, 27</sup>).
- $E_y \propto \exp(-i\omega t)$ .
- (23) Electron attachment is neglected and it is assumed that there are no negative ions present in the plasma.
- (24) The thermal DeBroglie wavelength of the electrons  $\lambda_{\text{DeBroglie}}$  is much less than the average particle spacing

$$\lambda_{\text{DeBroglie}} \ll N_e^{-1/3},$$

where

$N_e$  = electron particle density,

$$\lambda_{\text{DeBroglie}} = h/(2\pi m k T_e)^{1/2},$$

$h$  = Planck's constant,

$m$  = electron mass,

$k$  = Boltzmann's constant,

$T_e$  = electron temperature.

Then, the laws of classical physics can be used to describe the plasma.

- (25) The nonlinear force term

$$f_{\text{NL}} = -\frac{\partial}{\partial x} \left[ \frac{1}{2} \epsilon_0 |E_y|^2 + \frac{1}{2} \mu_0 |H_z|^2 \right] \quad (6)$$

discussed by Hora<sup>17</sup> affects only the electron momentum equation, but not the ion equation.

- (26) The term  $f_{\text{NL}} \cdot v_x$  is neglected in the energy equation for the electrons compared with the joule heating term  $J_y \cdot E_y$ , where  $J_y$  = ac current density, and  $v_x$  = electron velocity in the x direction.

26. Papa, R.J. (1965) Can. J. Physics 43:38.

27. Papa, R.J. (1968) Can. J. Physics, 46:889.

(27) The target is assumed not to melt, the target material passes directly from the solid to the vapor phase.

(28) Photo-ionization occurs only in the ambient gas, not in the target vapor.

(29) The nonlinear convective derivative terms are neglected in the momentum transfer equations for the electrons, target vapor ions, ambient gas ions and target vapor atoms. This permits the particle fluxes to be written in terms of appropriate diffusion coefficients multiplied by density and temperature gradients.

(30) The laser wave that is reflected from the target surface is neglected, there is only a wave travelling toward the target.

(31) The ambient gas ions are assumed to have the same temperature  $T_I$  as the ionized target vapor.

(32) The ac current density  $J_y^{ac}$  is made up of a component due to electron motion  $J_y^e$  and to the motion of the ambient gas ions  $J_y^I$ ; the current density due to the motion of the heavy target vapor ions is negligible:

$$J_y^{ac} = J_y^e + J_y^I.$$

With these assumptions, Maxwell's equations coupled with the fluid transport equations for the electrons, ions, neutral gas atoms, excited state atoms, target vapor ions, and neutral target vapor become (Holt and Haskell,<sup>16</sup> p. 156 et seq.):

$$\begin{aligned} \frac{\partial N_e}{\partial t} = & \nu_I N_e N_N + \nu_I^{ex} N_{ex} N_e + \nu_{IT} N_e N_T + \nu_{NNI} N_N (N_T + N_N) \\ & + \nu_{NNIT} N_T^2 + q N_N + q_{ex} N_{ex} - \alpha_r N_e (N_I + N_{IT}) - \frac{\partial \Gamma_e}{\partial x}. \end{aligned} \quad (7)$$

$$\frac{\partial N_{ex}}{\partial t} = D_{RAD} \frac{\partial^2 N_{ex}}{\partial x^2} + \nu_{ex} N_e N_N - \nu_I^{ex} N_e N_{ex} - N_{ex}/T^* - \frac{\partial \Gamma_{ex}}{\partial x}. \quad (8)$$

$$\begin{aligned} \frac{\partial N_I}{\partial t} = & \nu_I N_e N_N + \nu_I^{ex} N_{ex} N_e + \nu_{NNI} N_N (N_T + N_N) + q_{ex} N_{ex} + q N_N \\ & - \alpha_r N_e N_I - \frac{\partial \Gamma_I}{\partial x}. \end{aligned} \quad (9)$$

$$\frac{\partial N_{IT}}{\partial t} = \nu_{IT} N_e N_T + \nu_{NNIT} N_T^2 - \alpha_r N_e N_{IT} - \frac{\partial \Gamma_{IT}}{\partial x}. \quad (10)$$

$$\frac{\partial N_N}{\partial t} = -\nu_I N_e N_N - \nu_{NNI} N_N (N_T + N_N) - q N_N + \alpha_r N_e N_I - \nu_{ex} N_e N_N - \frac{\partial \Gamma_N}{\partial x} \quad (11)$$

$$\frac{\partial N_T}{\partial t} = -\nu_{IT} N_e N_T - \nu_{NNIT} N_T^2 + \alpha_r N_e N_{IT} + Q_T + D_T \frac{\partial^2 N_T}{\partial x^2} \quad (12)$$

$$\begin{aligned} \frac{\partial \Gamma_e}{\partial t} = & \frac{-\partial(\Gamma_e^2/N_e)}{\partial x} - \frac{1}{m} \frac{\partial(N_e k T_e)}{\partial x} - \frac{1}{m} \frac{\partial}{\partial x} \left[ \frac{1}{2} \epsilon_0 |E_y|^2 + \frac{1}{2} \mu_0 |H_z|^2 \right] \\ & - N_e \left( \frac{e}{m} \right) E_x + N_e \nu_{eN} (\Gamma_N/N_N) - \nu_{eN} \Gamma_e + N_e \nu_{eI} (\Gamma_I/N_I) - \nu_{eI} \Gamma_e \\ & + N_e \nu_{eex} (\Gamma_{ex}/N_{ex}) - \nu_{eex} \Gamma_e + N_e \nu_{eNT} (\Gamma_T/N_T) - \nu_{eNT} \Gamma_e \quad (13) \end{aligned}$$

$$\begin{aligned} \frac{\partial \Gamma_I}{\partial t} = & \frac{\partial(\Gamma_I^2/N_I)}{\partial x} - \frac{1}{m_I} \frac{\partial(N_I k T_I)}{\partial x} + N_I (e/m_I) E_x + N_I \bar{\nu}_{IN} (\Gamma_N/N_N) \\ & - \bar{\nu}_{IN} \Gamma_I + N_I \bar{\nu}_{Ie} (\Gamma_e/N_e) - \bar{\nu}_{Ie} \Gamma_I + N_I \bar{\nu}_{Iex} (\Gamma_{ex}/N_{ex}) - \bar{\nu}_{Iex} \Gamma_I \\ & + N_I \bar{\nu}_{INT} (\Gamma_T/N_T) - \bar{\nu}_{INT} \Gamma_I \quad (14) \end{aligned}$$

$$\begin{aligned} \frac{\partial \Gamma_{IT}}{\partial t} = & \frac{\partial(\Gamma_{IT}^2/N_{IT})}{\partial x} - \frac{1}{m_{IT}} \frac{\partial(N_{IT} k T_{IT})}{\partial x} + N_{IT} (e/m_{IT}) E_x + N_{IT} \bar{\nu}_{ITN} (\Gamma_N/N_N) \\ & - \bar{\nu}_{ITN} \Gamma_{IT} + N_{IT} \bar{\nu}_{ITe} (\Gamma_e/N_e) - \bar{\nu}_{ITe} \Gamma_{IT} \\ & + N_{IT} \bar{\nu}_{ITex} (\Gamma_{ex}/N_{ex}) - \bar{\nu}_{ITex} \Gamma_{IT} + N_{IT} \nu_{ITNT} (\Gamma_T/N_T) - \bar{\nu}_{ITNT} \Gamma_{IT} \quad (15) \end{aligned}$$

$$\Gamma_T = -D_T \frac{\partial N_T}{\partial x} \quad (16)$$

$$\begin{aligned}
\frac{\partial \Gamma_N}{\partial t} = & - \frac{\partial(\Gamma_N^2/N_N)}{\partial x} - \frac{1}{m_N} \frac{\partial(N_N k T_N)}{\partial x} + N_N \bar{\nu}_{Ne} (\Gamma_e/N_e) - \bar{\nu}_{Ne} \Gamma_N \\
& + N_N \bar{\nu}_{NI} (\Gamma_I/N_I) - \bar{\nu}_{NI} \Gamma_N + N_N \bar{\nu}_{Nex} (\Gamma_{ex}/N_{ex}) - \bar{\nu}_{Nex} \Gamma_N \\
& + N_N \bar{\nu}_{NNT} (\Gamma_T/N_T) - \bar{\nu}_{NNT} \Gamma_N .
\end{aligned} \quad (1')$$

$$\begin{aligned}
\frac{\partial \Gamma_{ex}}{\partial t} = & - \frac{\partial(\Gamma_{ex}^2/N_{ex})}{\partial x} - \frac{1}{m_N} \frac{\partial(N_{ex} k T_N)}{\partial x} + N_{ex} \bar{\nu}_{exe} (\Gamma_e/N_e) - \bar{\nu}_{exe} \Gamma_{ex} \\
& + N_{ex} \bar{\nu}_{exI} (\Gamma_I/N_I) - \bar{\nu}_{exI} \Gamma_{ex} + N_{ex} \bar{\nu}_{exN} (\Gamma_N/N_N) - \bar{\nu}_{exN} \Gamma_{ex} \\
& + N_{ex} \bar{\nu}_{exNT} (\Gamma_T/N_T) - \bar{\nu}_{exNT} \Gamma_{ex} .
\end{aligned} \quad (18)$$

$$\frac{\partial E_x}{\partial x} = (e/\epsilon_0) [N_I + N_{IT} - N_e] . \quad (19)$$

$$\begin{aligned}
\frac{\partial \left( \frac{3}{2} k N_e T_e \right)}{\partial t} + \frac{5}{2} k \frac{\partial(\Gamma_e \Gamma_e)}{\partial t} : \frac{1}{2} m \frac{\partial}{\partial t} (\Gamma_e^2/N_e) + \frac{1}{2} m \frac{\partial}{\partial x} (\Gamma_e^3/N_e^2) \\
- \frac{\partial}{\partial x} \kappa_e \frac{\partial T_e}{\partial x} = \langle E_y \cdot J_y^e \rangle_{AV} - G_{eN} N_e \frac{3}{2} k (T_e - T_N) \nu_{eN} \\
- G_{eI} N_e \frac{3}{2} k (T_e - T_I) \nu_{eI} - G_{eNT} N_e \frac{3}{2} k (T_e - T_T) \nu_{eNT} \\
- \nu_I N_e N_N E_I - \nu_I^{ex} N_{ex} N_e (E_I - E_{ex}) - \nu_{IT} N_e N_T E_{IT} \\
- \nu_{ex} N_e N_N E_{ex} - \alpha_r N_e (N_I + N_{IT}) \left( \frac{3}{2} k T_e \right) \\
- \left[ e^6 / (24 \pi \epsilon_0^3 c^3 m h) \right] \sqrt{(3/2) [8k/(\pi m)]^{1/2}} N_e^2 T_e^{1/2} \\
+ (q N_N + q_{ex} N_{ex}) (3 k T_e / 2) \\
+ \left[ \nu_{NII} N_N (N_I + N_N) + \nu_{NNT} N_T^2 \right] (3 k T_e / 2) .
\end{aligned} \quad (20)$$

$$\begin{aligned}
& \frac{\partial}{\partial t} \left( \frac{3}{2} N_I k T_I \right) + \frac{5}{2} k \frac{\partial}{\partial x} (T_I \Gamma_I) + \frac{1}{2} m_I \frac{\partial}{\partial t} (\Gamma_I^2 / N_I) + \frac{1}{2} m_I \frac{\partial}{\partial x} (\Gamma_I^3 / N_I^2) \\
& - \frac{\partial}{\partial x} \kappa_I \frac{\partial T_I}{\partial x} = \langle E_y \cdot J_y \rangle_{AV} + G_{eI} N_I \frac{3}{2} k (T_e - T_I) \nu_{eI} \\
& - G_{IN} N_I \frac{3}{2} k (T_I - T_N) \nu_{IN} - \alpha_r N_e (N_I + N_{IT}) \left( \frac{3}{2} k T_I \right) \\
& + (q N_N + q_{ex} N_{ex}) (3 k T_I / 2) \\
& + \left[ \nu_{NNI} N_N (N_T + N_N) + \nu_{NNIT} N_T^2 \right] (3 k T_I / 2) \\
& + \left( \frac{1}{12} \right) \sqrt{\pi} \left( \frac{m v_E^4}{c^2} \right) \left( \frac{1}{\omega} \right) \left( \frac{\omega}{\Delta \omega} \right) (c k_L)^3 \left( \frac{m_I}{m} \right)^{1/2} \\
& \times N_e \frac{T_0^{3/2} T_I^{1/2}}{(T_e + T_I)^2} \left[ \frac{a^2 (2 + 6a^2 + 3a^4)}{(2 + a^2)} + \left( \frac{a}{\sqrt{2}} \right) (2 - 2a^2 - 3a^4) \right. \\
& \left. \times \tan^{-1} (\sqrt{2}/a) \right] . \tag{21}
\end{aligned}$$

$$\begin{aligned}
& \frac{3}{2} k \frac{\partial (N_T T_T)}{\partial t} = - \frac{5}{2} k \frac{\partial}{\partial x} (\Gamma_T T_T) + \kappa_T \frac{\partial^2 T_T}{\partial x^2} \\
& + \frac{3}{2} k G_{eNT} N_e (T_e - T_T) \nu_{eNT} + \frac{3}{2} k G_{NNT} N_N (T_N - T_T) \nu_{NNT} \\
& - \nu_{IT} N_e N_T \left( \frac{3}{2} k T_T \right) + \alpha_r N_e N_{IT} \left( \frac{3}{2} k T_T \right) \\
& - \nu_{NNIT} N_T^2 \left( \frac{3}{2} k T_T \right) + \frac{3}{2} k Q_T T_T (x = L) . \tag{22}
\end{aligned}$$

$$\begin{aligned}
& \frac{\partial}{\partial t} \left( \frac{3}{2} k N_N T_N \right) + \frac{5}{2} k \frac{\partial}{\partial x} (T_N \Gamma_N) + \frac{1}{2} m_N \frac{\partial}{\partial t} (\Gamma_N^2 / N_N) + \frac{1}{2} m_N \frac{\partial}{\partial x} (\Gamma_N^3 / N_N^2) \\
& - \frac{\partial}{\partial x} \kappa_N \frac{\partial T_N}{\partial x} = G_{eN} N_e \frac{3}{2} k (T_e - T_N) \nu_{eN} + G_{IN} N_e \frac{3}{2} k (T_I - T_N) \nu_{IN} \\
& + G_{NNT} N_N (T_T - T_N) \nu_{NNT} - \nu_I N_e N_N (3 k T_N / 2) + \tag{23}
\end{aligned}$$

$$\begin{aligned}
& - \nu_{NNI} N_N (N_T + N_N) (3 k T_N / 2) - \nu_{ex} N_e N_N \left( \frac{3}{2} k T_N \right) \\
& + \alpha_r N_e N_I \left( \frac{3}{2} k T_N \right) - [q N_N + q_{ex} N_{ex}] (3 k T_N / 2) \quad . \quad (23 \text{ contd})
\end{aligned}$$

$$\frac{\partial E_y}{\partial x} = i \omega \mu_0 H_z \quad . \quad (24)$$

$$\frac{\partial H_z}{\partial x} = i \omega \epsilon_0 E_y - J_y^e - J_y^I \quad . \quad (25)$$

$$J_y^e = -e N_e v_y^e \quad . \quad (26)$$

$$J_y^I = e N_I v_y^I \quad . \quad (27)$$

$$\frac{\partial (N_e v_y^e)}{\partial t} + \frac{\partial}{\partial x} (N_e v_x^e v_y^e) + N_e \left( \frac{e}{m} \right) E_y = -N_e \nu_{eN} v_y^e + N_e \nu_{eI} (v_y^I - v_y^e) \quad . \quad (28)$$

$$\frac{\partial (N_I v_y^I)}{\partial t} + \frac{\partial}{\partial x} (N_I v_x^I v_y^I) - N_I \left( \frac{e}{m_I} \right) E_y = -N_I \bar{\nu}_{IN} v_y^I + N_I \bar{\nu}_{Ie} (v_y^e - v_y^I) \quad . \quad (29)$$

Here, the laser wave propagates in the + x direction and the target is located at  $x = L$ .

$$E_y \text{ and } H_z \propto \exp(-i \omega t) \quad .$$

$N_j$  = particle number density.

$j$  = e  $\rightarrow$  electrons.

= I  $\rightarrow$  ambient gas ions.

= IT  $\rightarrow$  target vapor ions.

= N  $\rightarrow$  ambient gas atoms.

= NT  $\rightarrow$  target vapor atoms.

= ex  $\rightarrow$  excited state atoms.

$\Gamma_j$  = flux density of species j.



$T_j$	= temperature of species j.
$\nu_I$	= ionization frequency due to electron impact on ambient gas atoms (ionization cross section, times relative velocity).
$\nu_{IT}$	= ionization frequency due to electron impact on target vapor atoms.
$\nu_{NNI}$	= ionization frequency due to a neutral atom colliding with an ambient gas atom.
$\nu_{NNIT}$	= ionization frequency due to a neutral atom colliding with a target vapor atom.
$\nu_I^{ex}$	= ionization frequency due to electron impact on an excited state atom.
$\alpha_r$	= total recombination rate coefficient for radiative recombination and electron-electron-ion recombination.
$q$	= photo-ionization rate for ionization of ambient gas atoms by continuum radiation.
$q_{ex}$	= photo-ionization rate for ionization of excited state atoms by continuum radiation.
$D_{RAD}$	= diffusion coefficient for resonant radiation (bound-bound transitions) = $(l^2/3\tau)$ .
$l$	= mean free path of resonant radiation quanta.
$\tau$	= average lifetime of excited atomic state.
$\nu_{ex}$	= rate coefficient for production of excited states by electron impact on ambient gas atoms.
$\tau^*$	= average time for resonant radiation to escape from plasma (laterally, in y-z plane).
$k$	= Boltzmann's constant.
$m_j$	= particle mass of species j.
$m = m_e$	= electron mass.
$E_y$	= ac electric field of laser wave.
$H_z$	= ac magnetic field of laser wave.
$N_T$	= particle density of target vapor.
$e$	= charge on electron.
$v_y^j$	= particle velocity in y direction of species j.
$v_x^j$	= particle velocity in x direction of species j.

$\epsilon_0$	= permittivity of free space.
$\mu_0$	= permeability of free space.
$\Gamma_j$	= $N_j v_x^j$ .
$E_x$	= quasi-static electric field due to charge separation.
$\nu_{eN}$	= electron-neutral collision frequency for momentum transfer.
$\nu_{eI}$	= electron-ion collision frequency.
$\nu_{kj}$	= collision frequency for momentum transfer between species k and species j.
$\bar{\nu}_{kj}$	= $\nu_{kj} m_j / (m_k + m_j)$ . = collision frequency for momentum transfer between species k and species j transformed from center of mass coordinates to laboratory coordinates.
$K_j$	= thermal conductivity of gas consisting of species j.
$G_{kj}$	= fractional energy loss in collisions between species k and species j = $2m_k m_j / (m_k + m_j)^2$ for elastic collisions between species k and species j.
$c$	= velocity of light.
$h$	= Planck's constant.
$E_I$	= ionization energy of ambient gas from ground state.
$E_{IT}$	= ionization energy of target material.
$E_{ex}$	= energy of excited atomic state.
$Q_T$	= rate of emission of target vapor at target surface, = $N_T \nu_0 \exp [-LM/N_0 kT_T (x = L)]$ .
$\nu_0$	= Debye frequency.
$M$	= atomic weight of target material.
$N_0$	= Avogadro's number.
$D_T$	= diffusion coefficient for target vapor, = $kT_T / (m_T \bar{\nu}_{NTN})$ .
$J_y^k$	= ac current density of species k.
$v_E$	= $c  E_y  / (m\omega)$ .
$\omega$	= frequency of laser radiation.

$$\begin{aligned}
k_L &= \sqrt{\omega^2 - \omega_p^2} \\
\omega_p^2 &= \text{square of plasma frequency} = N_e e^2 / (m \epsilon_0) \\
\Delta\omega/\omega &= \text{relative frequency spread of laser radiation.} \\
T_0 &= (mc^2 / 8k) (\Delta\omega/\omega)^2 \\
a^2 &= \frac{1}{2} (mc^2 / kT_e) (\omega_p^2 / (\omega^2 - \omega_p^2)) (1 + T_e/T_i)
\end{aligned}$$

The physical significance of each term in Eqs. (7) through (29) is discussed in reference (9). In reference 9, it was explained how additional assumptions are made to further simplify Eqs. (7) through (29). The terms

$$v_y^e \frac{\partial N_e}{\partial t}$$

and

$$\frac{\partial}{\partial x} [N_e v_x^e v_y^e]$$

in Eq. (28) for the y component of the electron velocity are small and can be neglected if it is assumed that:

(33) The time scale for electron-density changes  $\tau_{N_e}$  is long compared with a wave period

$$\tau_{N_e} \gg (2\pi/\omega) \quad .$$

(34) The electron-neutral collision frequency  $\nu_{eN}$  or the electron-ion collision frequency  $\nu_{eI}$  is large compared with  $v_x^e / L_{N_e}$ , where  $L_{N_e}$  is the space scale for electron density gradients

$$\nu_{eN} \gg v_x^e / L_{N_e}$$

or

$$\nu_{eI} \gg v_x^e / L_{N_e} \quad .$$

Similar assumptions can be made in Eq. (29) for the y component of the ion velocity:

(35) It is assumed that the time scale for ion-density changes  $\tau_{N_I}$  is long compared with a wave period

$$\tau_{N_I} \gg (2\pi/\omega) \quad .$$

(36) It is assumed that the ion-neutral collision frequency  $\bar{\nu}_{IN}$  or the ion-electron collision frequency  $\bar{\nu}_{Ie}$  be large compared with  $v_x^I/L_{NI}$ , where  $L_{NI}$  is the space scale for ion-density changes

$$\bar{\nu}_{IN} \gg v_x^I/L_{NI}$$

or

$$\bar{\nu}_{Ie} \gg v_x^I/L_{NI}.$$

With assumptions (33) through (35), Eqs. (28) and (29) become:

$$-i\omega v_y^e + \frac{e}{m} E_y = -\nu_{eN} v_y^e + \nu_{eI} (v_y^I - v_y^e) \quad (30)$$

$$-i\omega v_y^I - \left(\frac{e}{m_I}\right) E_y = -\bar{\nu}_{IN} v_y^I + \bar{\nu}_{Ie} (v_y^e - v_y^I) \quad (31)$$

Solving Eqs. (30) and (31) yields:

$$v_y^e = \frac{+eE_y(\omega - \bar{\nu}_{IN})}{m \cdot \text{DENOM}} \quad (32)$$

$$v_y^I = \frac{-eE_y(\omega - \nu_{eN})}{m_I \cdot \text{DENOM}} \quad (33)$$

where

$$\text{DENOM} = -\omega^2 - i\omega(\nu_{eN} + \nu_{eI} + \bar{\nu}_{IN} + \bar{\nu}_{Ie}) + \nu_{eN}\bar{\nu}_{IN} + \nu_{eN}\bar{\nu}_{Ie} + \nu_{eI}\bar{\nu}_{IN}.$$

The self-consistent electric field  $E_x$  that appears in Eqs. (13), (14), (15), and (19) may be eliminated by making several additional assumptions. The initial ionization is assumed to be sufficiently high that the Debye length  $l_D$  is much less than the scale lengths  $L_{Ne}$  and  $L_{NI}$  for electron and ion density changes:

$$(37) \quad l_D \ll L_{Ne} \text{ or } L_{NI}$$

where

$$l_D^{-2} = \left(e^2/\epsilon_0 k\right) \left[ \frac{N_e}{T_e} + \frac{(N_I + N_{IT})}{T_I} \right].$$

From Poisson's Eq. (19) and assumption (37) it is easily shown that

$$N_e = N_I + N_{IT} \quad (34)$$

for distances greater than a Debye length. Then, subtracting Eqs. (9) and (10) from Eq. (7) and using Eq. (34) gives:

$$\frac{\partial \Gamma_e}{\partial x} = \frac{\partial \Gamma_I}{\partial x} + \frac{\partial \Gamma_{IT}}{\partial x} \quad (35)$$

From assumption (19) one may deduce that the plasma is irrotational, so that Eq. (35) implies that

$$\Gamma_e = \Gamma_I + \Gamma_{IT} \quad (36)$$

In order to simplify Eqs. (13), (14), and (15), the self-consistent electric field  $E_x$  may be eliminated by making the following assumptions:

$$(38) \quad \frac{\partial \Gamma_e}{\partial t} \ll \nu_{eN} \Gamma_e \quad .$$

$$(39) \quad \nu_{eI} \ll \nu_{eN} \quad .$$

$$(40) \quad \nu_{eex} \ll \nu_{eN} \quad .$$

$$(41) \quad \nu_{eNT} \ll \nu_{eN} \quad .$$

$$(42) \quad \frac{\partial \Gamma_I}{\partial t} \ll \bar{\nu}_{IN} \Gamma_I \quad .$$

$$(43) \quad \bar{\nu}_{Ie} \ll \bar{\nu}_{IN} \quad .$$

$$(44) \quad \bar{\nu}_{Iex} \ll \bar{\nu}_{IN} \quad .$$

$$(45) \quad \bar{\nu}_{INT} \ll \bar{\nu}_{IN} \quad .$$

$$(46) \quad \frac{\partial \Gamma_{IT}}{\partial t} \ll \nu_{ITN} \Gamma_{IT} \quad .$$

$$(47) \quad \bar{\nu}_{ITe} \ll \bar{\nu}_{ITN} \quad .$$

$$(48) \quad \bar{\nu}_{Iex} \ll \bar{\nu}_{ITN} \quad .$$

$$(49) \bar{v}_{INT} \ll \bar{v}_{ITN} .$$

Also, it was shown in reference 9, p. 54, that

$$(50) v_x^e \ll \sqrt{(3kT_e)/m} ,$$

which implies that

$$(51) v_x^I \ll [3kT_I/m_I]^{1/2}$$

and

$$v_x^{IT} \ll [3kT_I/m_{IT}]^{1/2} .$$

The use of assumptions (38) through (51) permits the reduction and simplification of Eqs. (13), (14), and (15) to the following form:

$$-\bar{v}_e N^I_e = \frac{1}{m} \frac{\partial(N_e kT_e)}{\partial x} + \frac{N_e e E_x}{m} + \frac{1}{m} \frac{\partial}{\partial x} \left[ \frac{1}{2} \epsilon_0 |E|^2 + \frac{1}{2} \mu_0 |H|^2 \right] . \quad (37)$$

$$-\bar{v}_{IN} \Gamma_I = \frac{1}{m_I} \frac{\partial}{\partial x} (N_I kT_I) - \frac{N_I e E_x}{m_I} . \quad (38)$$

$$-\bar{v}_{ITN} \Gamma_{IT} = \frac{1}{m_{IT}} \frac{\partial}{\partial x} (N_{IT} kT_I) - \frac{N_{IT} e E_x}{m_{IT}} . \quad (39)$$

The use of Eq. (36) allows  $E_x$  to be eliminated from Eqs. (37), (38), and (39). From the computer runs made in reference 9, it can be shown that

$$(52) \frac{1}{N_e} \frac{\partial N_e}{\partial x} \gg \frac{1}{T_e} \frac{\partial T_e}{\partial x} , \text{ and}$$

$$(53) \frac{1}{N_I} \frac{\partial N_I}{\partial x} \gg \frac{1}{T_I} \frac{\partial T_I}{\partial x} .$$

Then, also assuming that

$$(54) \frac{1}{N_{IT}} \frac{\partial N_{IT}}{\partial x} \gg \frac{1}{T_I} \frac{\partial T_I}{\partial x} .$$

it is possible to solve Eqs. (37), (38), and (39), after eliminating  $E_x$ , to obtain the results:

$$\Gamma_e = -\text{DIFFE}_1 \frac{\partial N_e}{\partial x} - \text{DIFFE}_2 \frac{\partial N_{IT}}{\partial x} - \text{ANLP} \frac{\partial}{\partial x} \left[ \frac{1}{2} \epsilon_0 |E|^2 + \frac{1}{2} \mu_0 |H|^2 \right] ; \quad (40)$$

$$\Gamma_{IT} = -\text{DIFFIT}_1 \frac{\partial N_{IT}}{\partial x} - \text{DIFFIT}_2 \frac{\partial N_e}{\partial x} - \text{ANLPI} \frac{\partial}{\partial x} \left[ \frac{1}{2} \epsilon_0 |E|^2 + \frac{1}{2} \mu_0 |H|^2 \right] ; \quad (41)$$

where

$$\text{DIFFE}_1 = \left( \frac{1}{\text{DEN}} \right) \left( \frac{k}{m} \right) \left[ \frac{\bar{v}_{ITN}}{m_I} (T_e + T_I) + \left( \frac{N_{IT}}{N_e} \right) T_e \left( \frac{\bar{v}_{IN}}{m_{IT}} - \frac{\bar{v}_{ITN}}{m_I} \right) \right] ,$$

$$\text{DEN} = \left( \frac{N_{IT}}{N_e} \right) \nu_{eN} \left[ \frac{\bar{v}_{IN}}{m_{IT}} - \frac{\bar{v}_{ITN}}{m_I} \right] + \bar{v}_{ITN} \left[ \nu_{eN}/m_I + \bar{v}_{IN}/m \right] ,$$

$$\text{DIFFE}_2 = (1/\text{DEN}) [kT_I/m] \left[ \frac{\bar{v}_{IN}}{m_{IT}} - \frac{\bar{v}_{ITN}}{m_I} \right] ,$$

$$\text{ANLP} = \left( \frac{1}{m \cdot \text{DEN}} \right) \left[ \frac{\bar{v}_{ITN}}{m_I} + \left( \frac{N_{IT}}{N_e} \right) \left( \frac{\bar{v}_{IN}}{m_{IT}} - \frac{\bar{v}_{ITN}}{m_I} \right) \right] ,$$

$$\text{DIFFIT}_1 = (1/\text{DEN}) (kT_I/m_{IT}) \left( \frac{\nu_{eN}}{m_I} + \frac{\bar{v}_{IN}}{m} \right) ,$$

$$\text{DIFFIT}_2 = (1/\text{DEN}) \left( \frac{k N_{IT}}{m_{IT} N_e} \right) \left[ \frac{\bar{v}_{IN} T_e}{m} - \frac{\nu_{eN} T_I}{m_I} \right] ,$$

$$\text{ANLPI} = (1/\text{DEN}) \left( \frac{N_{IT}}{m N_e} \right) (\bar{v}_{IN}/m_{IT}) .$$

When  $N_{IT} \rightarrow 0$ ,

then  $\Gamma_{IT} \rightarrow 0$  and

$$\Gamma_e \rightarrow - \frac{k(T_e + T_I)}{m_I \bar{v}_{IN}} \frac{\partial N_e}{\partial x} ,$$

which is the usual expression for ambipolar diffusion in the presence of a single positive ion species.

Substituting Eqs. (32) and (33) into Eqs. (26) and (27), and then substituting Eqs. (26) and (27) into Eq. (25) gives

$$\frac{\partial H_z}{\partial x} = \left[ i\omega\epsilon_0 + \frac{N_e e^2 (\omega - \bar{\nu}_{IN})}{m \cdot \text{DENOM}} + \frac{N_e e^2 (\omega - \nu_{eN})}{m_I \cdot \text{DENOM}} \right] E_y . \quad (42)$$

It is reasonable to assume that the scale length for electron density changes

$$L_{N_e} = \left[ \frac{\partial \ln N_e}{\partial x} \right]^{-1}$$

is long compared with the laser wavelength  $\lambda_p$  in the plasma produced in front of the target:

$$(55) \quad L_{N_e} \gg \lambda_p .$$

It is convenient to rewrite Eq. (42) in the form

$$\frac{\partial H_z}{\partial x} = i\omega\epsilon_0 E_y - \sigma E_y = i\omega\epsilon_0 K E_y , \quad (43)$$

where  $\sigma$  the conductivity, is given by

$$\sigma = - \frac{N_e e^2}{\text{DENOM}} \left[ \frac{(i\omega - \bar{\nu}_{IN})}{m} + \frac{(i\omega - \nu_{eN})}{m_I} \right] ,$$

and the dielectric constant  $K$  is given by

$$K = 1 - \frac{\sigma}{(i\omega\epsilon_0)} .$$

Combining Eqs. (42) and (24) yields the wave equation

$$\frac{\partial^2 E_y}{\partial x^2} + \frac{\omega^2}{c^2} K E_y = 0 . \quad (44)$$

Since the electron density  $N_e$  and electron temperature  $T_e$  are functions of the electric field intensity  $E_y$ , and since  $K$  is a function of  $N_e$  and  $T_e$ , Eq. (44) is



nonlinear in  $E_y$ . However, the use of assumption (55) permits Eq. (44) to be solved using the WKB perturbation method (Ginzburg, <sup>28</sup> chapter 39):

$$E_y = \frac{E_{INC}}{K^{1/4}} \exp \left[ i \left( \frac{\omega}{c} \right) \int_{x_0}^x \sqrt{K} dx \right] , \quad (45)$$

where  $E_{INC}$  is the incident field intensity at position  $x = x_0$ .

Thus, under these 55 assumptions, the transport equations coupled with Maxwell's equations reduce to Eqs. (7), (8), (9), (10), (11), (12), (16), (17), (18), (20), (21), (22), (23), (24), (34), (36), (40), (41), and (45). It should be noted that the terms

$$\frac{1}{2} m \frac{\partial}{\partial t} \left( \Gamma_e^2 / N_e \right) \text{ and } \frac{1}{2} m \frac{\partial}{\partial x} \left( \Gamma_e^3 / N_e^2 \right)$$

can be deleted from Eq. (20), because it was shown in reference 9 that

$$v_x^e \ll [3kT_e / \ln]^{1/2} .$$

As indicated in reference 9, the electron temperature  $T_e$ , the electron flux density  $\Gamma_e$ , and indirectly, the electron density  $N_e$ , ionization frequency  $\nu_i$ , electron thermal conductivity  $K_e$ , target temperature  $T_T$  ( $x = L$ ), target vapor density  $N_T$ , and so forth, are all functions of the electromagnetic field intensity  $|E_y|$ . This implies that all particle densities and temperatures are mutually coupled. The system of nonlinear, partial differential equations is solved by converting them to a system of partially implicit, partially explicit (PI - PE) difference equations. <sup>21</sup>

The boundary conditions are such that the target temperature  $T_T$  ( $x = L$ ) is given by Eq. (1), but  $T_T$  ( $x = L$ ) cannot exceed  $T'$  given by Eq. (5). The target vapor density  $N_T$ , at the target surface  $x = L$ , is given by the expression

$$N_T(x = L) = \int_{t'=0}^{t'=t} dt' \left[ N_{TS} \nu_0 \exp(-LM/N_0 k T_T(x = L)) + D_T \frac{\partial^2 N_T(x = L)}{\partial x^2} \right] , \quad (46)$$

where  $N_{TS}$  = target material density at target surface. The momentum and energy transfer terms in the transport equations are set up in such a fashion that the total

28. Ginzburg, V.L. (1964) The Propagation of Electromagnetic Waves in Plasmas, Pergamon Press.

momentum and energy of the entire system is conserved. Also, the gain and loss terms in the continuity equations are such that the total particle density is conserved. Thus, there is no need to impose particle, momentum, and energy conservation conditions at the boundaries of the system. The boundary conditions on the dependent variables  $N_e$ ,  $N_{ex}$ ,  $N_N$ ,  $N_I$ ,  $\Gamma_N$ ,  $\Gamma_{ex}$ ,  $T_e$ ,  $T_I$ , and  $T_N$  are free. The electromagnetic field quantities  $E_y$  and  $H_z$  are specified at  $x = -\infty$  (laser wave source). The solution to the laser-target interaction problem is determined with the specification of the initial conditions on the dependent variables  $N_e$ ,  $N_{ex}$ ,  $N_N$ ,  $N_I$ ,  $N_T$ ,  $\Gamma_N$ ,  $\Gamma_{ex}$ ,  $T_e$ ,  $T_I$ ,  $T_N$ , and  $T_T$  for  $-\infty < x < +\infty$ .

In this report, the background gas is taken to be xenon. The transport coefficients, reaction rate coefficients, and cross sections have been selected from a number of references. A list of the physical constants and transport coefficients follows:

$\nu_I$  = ionization frequency for electrons impacting on the neutral particles in the ground state,

$$\nu_I = 8kT_e/(\pi m)]^{1/2} (\pi a_0^2) \exp(-E_I/kT_e) ,$$

$E_I$  = ionization energy of ambient gas atoms (xenon)

$$= 19.408 \times 10^{-19} \text{ joules,}$$

$$= \text{Bohr radius} = 0.53 \times 10^{-10} \text{ m.}$$

This expression for  $\nu_I$  was taken from Lin and Teare.<sup>29</sup>

$\nu_{IT}$  = ionization frequency due to electron impact on target vapor atoms,

$$= 8kT_e/(\pi m)]^{1/2} (\pi a_0^2) \exp(-E_{IT}/kT_e) .$$

$E_{IT}$  = ionization energy of target vapor,

$$= 5.984 \times 1.6 \times 10^{-19} \text{ joules.}$$

$\nu_{NNI}$  = ionization frequency due to a neutral atom colliding with an ambient gas atom,

$$= 10^{-22} [8kT_N/(\pi m_N)]^{1/2} [E_I/(kT_N) + 1] \cdot \exp(-E_I/kT_N) .$$

This expression for  $\nu_{NNI}$  was taken from Zeldovich and Raizer.<sup>30</sup>

$\nu_{NNIT}$  = ionization frequency due to a neutral atom colliding with a target vapor atom,

$$= 10^{-22} [8kT_T/(\pi m_T)]^{1/2} \cdot [E_{IT}/(kT_T) + 1] \cdot \exp[-E_{IT}/kT_T] .$$

29. Lin, S. C. and Teare, J. D. (1962) Avco Research Report 115, Contract No. AF19(604)-7458.

30. Zeldovich, Ya. B. and Raizer, Yu. P. (1966) Physics of Shock Waves and High-Temperature Hydrodynamic Phenomena, Vol. 1, Academic Press.

$$\nu_I^{\text{ex}} = \text{ionization frequency due to electron impact on an excited state atom,} \\ = [8kT_e / (\pi m)]^{1/2} (\pi a_0^2) \cdot \exp - [(E_1 - E_{\text{ex}})/kT_e].$$

$$E_{\text{ex}} = \text{excited state energy,} \\ = 14.4 \times 10^{-19} \text{ joules.}$$

$$\alpha_r = \text{total recombination rate coefficient for radiative recombination and} \\ \text{electron-electron-ion recombination (from analogous calculations} \\ \text{performed for hydrogen, as given in McDaniel}^{31}).$$

$$q = \text{photoionization rate for ionization of ambient gas atoms by continuum} \\ \text{radiation,} \\ = 4\pi \int I_\nu (1/h\nu) \sigma_{\nu n} (1 - e^{-y}) d\nu ,$$

where

$$y = h\nu / (kT_N),$$

$$\nu = \text{frequency of continuum radiation,}$$

$$I_\nu = \text{spectral intensity of continuum radiation,}$$

$$\sigma_{\nu n} = \text{cross section for the absorption of a photon } h\nu \text{ by an atom in the } n\text{th} \\ \text{state and removal of an electron.}$$

This expression for  $q$  is given by Zeldovich and Raizer.<sup>30</sup> For a hydrogen-like atom whose remainder charge is  $Z$  in the  $n$ th quantum state

$$\sigma_{\nu n} = 7.9 \times 10^{-22} (n/Z^2)(\nu/\nu_n)^3 , \quad \text{in meters squared} ,$$

where  $\nu_n$  is the minimum frequency of a photon still capable of removing an electron from the  $n$ th level (Kramer's formula).

For the steady state case, where the temperature, density distribution, and radiation field are in local thermodynamic equilibrium, the spectral intensity is given by

$$I_\nu(x) = \int_{x_0}^x K'_\nu I_{\nu p} \exp \left[ - \int_{x'}^x K'_\nu dx'' \right] dx' + I_{\nu 0} \exp \left[ - \int_{x_0}^x K'_\nu dx'' \right] ,$$

31. McDaniel, E. W. (1964) Collision Phenomena in Ionized Gases, John Wiley and Sons.

where

$$\begin{aligned}
 I_{\nu 0} &= \text{intensity of any incident external radiation,} \\
 K'_{\nu} &= \text{absorption coefficient lowered by induced emission,} \\
 K'_{\nu} &= K_{\nu} [1 - \exp(-h\nu/kT_N)] \quad , \\
 K_{\nu} &= \text{absorption coefficient,} \\
 I_{\nu p} &= \text{Planck distribution for radiative equilibrium,} \\
 &= (2h\nu^3/c^2) \left[ \frac{1}{\exp(h\nu/kT_N) - 1} \right] \quad .
 \end{aligned}$$

For continuous absorption of light in inert monatomic gases when  $h\nu > E_I$ , an approximate expression for  $K_{\nu}$  is given by

$$K_{\nu} = 0.96 \times 10^{-11} \left( \frac{N_N}{T_N^2} \right) \left( \frac{2y_1}{y^3} \right) \quad , \quad \text{in inverse meters} \quad ,$$

where

$$\begin{aligned}
 y_1 &= E_I/kT_N \quad , \\
 y &= h\nu/kT_N \quad .
 \end{aligned}$$

When the plasma in front of the target is sufficiently hot to radiate appreciably, then  $K_{\nu} \gg 1$  (the plasma is optically thick to the continuum radiation). In this case,

$$\begin{aligned}
 q &= 4 \int I_{\nu p} \left( \frac{1}{h\nu} \right) \sigma_{\nu 1} (1 - e^{-y}) d\nu \quad , \\
 &= 4 \left( \frac{1}{h} \right) 7.9 (10^{-22}) \frac{2E_I^3}{(hc)^2} \cdot \int_{y_1}^{\infty} \frac{(1 - e^{-y})}{(e^y + 1)y} dy \quad , \\
 &\cong 4(1/h) 7.9 (10^{-22}) \frac{2E_I^3}{(hc)^2} \frac{e^{-y_1}}{y_1} \left( 1 + \frac{1}{y_1} \right) \quad .
 \end{aligned}$$

$q_{\text{ex}}$  = photo-ionization rate for ionization of excited state atoms by continuum radiation,

$$= 8(1/h) 7.9 (10^{-22}) \frac{2(E_I - E_{\text{ex}})^3}{(hc)^2} \frac{e^{-y_{\text{ex}}}}{y_{\text{ex}}} \left( 1 + \frac{1}{y_{\text{ex}}} \right) \quad .$$

$$y_{ex} = (E_I - E_{ex})/kT_N .$$

While the continuum radiation is such that the plasma appears optically thick, the resonant line radiation can diffuse because of the finite line-width. The following expressions describing the transport processes of the "wings" of the resonant radiation line are taken from Myshekov and Raizer.<sup>25</sup>

$$D_{RAD} = l^2/(3\tau),$$

= effective resonant radiation diffusion coefficient,

$l$  = mean-free path of resonant radiation quanta,

$$l^2 = 0.7901 \times 10^{-7} \text{ m},$$

$\tau$  = average lifetime of excited state,

$$= 3.74 \times 10^{-9} \text{ sec.}$$

$T^*$  = average time for resonant radiation to escape from plasma (laterally, in y - z plane),

$$= (R^2/3 D_{RAD}).$$

$R$  = average distance from center of plasma to lateral boundary (approx. 0.01 m).

$\nu_{ex}$  = collision frequency for production of excited state atoms due to electron impact on ambient gas atoms.

$$\nu_{ex} = \int_{v_{ex}}^{\infty} v^3 \sigma_{ex} f_0 4\pi dv ,$$

$$= 10^{-22} (2/\sqrt{\pi}) \beta_e^{1/2} \cdot \exp(-\beta_e v_{ex}^2) [v_{ex}^2 + 1/\beta_e] .$$

$f_0$  = Maxwellian electron distribution function,

$$= \left( m_e / (2\pi kT_e) \right)^{3/2} \exp[-mv^2/(2kT_e)] .$$

$$v_{ex} = \sqrt{2E_{ex}/m} .$$

$v$  = electron velocity.

$\sigma_{ex}$  = cross section for excitation,

$$= 10^{-22} \text{ m}^2 \text{ (from Massey et al. }^{32}\text{)}.$$

$$\beta_e = m/(2kT_e).$$

32. Massey, H. S. W., Burhop, E. H. S., and Gilbody, H. B. (1969) Electronic and Ionic Impact Phenomena, Oxford Clarendon Press.

$\nu_{eN}$  = electron-neutral collision frequency for momentum transfer,

$$= N_N 4\pi (m_e/2\pi kT_e)^{3/2} \int_0^\infty \sigma_{eN} v^3 \exp[-\beta_e v^2] dv,$$

$$= (6/\sqrt{\pi})(10^{-18})\beta_e^{-1/2} N_N.$$

$\sigma_{eN}$  = momentum transfer cross section,

$$= 3(10^{-18}) \text{ m}^2 \text{ (from Massey et al. }^{32}\text{)}.$$

$\nu_{eI}$  = electron-ion collision frequency,

$$\nu_{eI} = \frac{N_e (\ln \Lambda) T_e^{-3/2}}{0.38} (10^{-6}) \text{ (from Holt and Haskell }^{16}\text{)}.$$

$$\Lambda = l_D/p_c.$$

$$p_c = 5.55(10^{-6}) T_e^{-1}.$$

$$l_D = 69.0 (T_e/N_e)^{1/2}.$$

$\nu_{IN}$  = ion-neutral collision frequency,

$$= N_N \sigma_{IN} v_I.$$

$$v_I = [3kT_I/m_I]^{1/2}.$$

$\sigma_{IN}$  = cross section for momentum transfer,

$$= e/(m_I \mu_{IN} N_N v_I).$$

$\mu_{IN}$  = mobility,

$$= 0.6(10^{-4}) \text{ m}^2/(\text{volt-sec}) \text{ (from McDaniel }^{31}\text{)}.$$

$\nu_{eex}$  = collision frequency for electron-excited state atoms,

$$= \nu_{eN}(N_{ex}/N_N).$$

$\nu_{Iex}$  = ion-excited state collision frequency,

$$= \nu_{IN}(N_{ex}/N_N).$$

$\nu_{ITN}$  = target vapor ion-neutral gas collision frequency.

$$= N_N \sigma_{IN} v_{IT}.$$

$$v_{IT} = \sqrt{3kT_I/m_{IT}}.$$

$\nu_{NTN}$  = target vapor-neutral gas collision frequency,

$$= N_N (\pi a_0^2) v_{NT}.$$

$$v_{NT} = \sqrt{3kT_T/m_T}.$$

$$K_N = \text{thermal conductivity of ambient gas,} \\ = (1/2)(8kT_N/\pi m_N)^{1/2} \frac{k}{\sqrt{2}(4\pi a_0^2)} .$$

$$K_T = \text{thermal conductivity of target vapor,} \\ = (1/2)(8kT_T/\pi m_T)^{1/2} \frac{k}{\sqrt{2}(4\pi a_0^2)} .$$

$$K_e = \text{electron thermal conductivity,} \\ = \frac{5N_e k^2 T_e}{m \nu_{eI}} \text{ (from Shkarofsky et al. }^{33}\text{).}$$

$$K_I = \text{ion thermal conductivity,} \\ K_I = \frac{5N_e k^2 T_i}{m_I \left[ \nu_{eI} (m/m_I)^{1/2} (T_e/T_i)^{3/2} \right]} \text{ (from Shkarofsky et al. }^{33}\text{).}$$

$$m_T = \text{target atom mass,} \\ = 4.514 \times 10^{-26} \text{ kg (aluminum).}$$

$$c_p = \text{specific heat of target material,} \\ = 0.9 \times 10^3 \text{ joules/(kg} \cdot ^\circ\text{K) (aluminum).}$$

$$L = \text{heat of vaporization,} \\ = 1.076 \times 10^7 \text{ joules/kg.}$$

$$\rho = \text{density of aluminum,} \\ = 5.986 \times 10^{28} \text{ kg/m}^3 .$$

$$G_{eN} = \text{relative fractional energy loss for elastic electron - neutral collisions,} \\ = 2m_e/m_N .$$

$$G_{eI} = G_{eN} .$$

$$G_{IN} = \frac{2m_I m_N}{(m_I + m_N)^2} = 1/2 .$$

$$Q_T = \text{rate of emission of target vapor at target surface,} \\ = N_T(x = L) \nu_0 \exp [-LM/N_0 k T_T(x = L)] .$$

33. Shkarofsky, I.P., Johnston, T.W., and Bachynski, M.P. (1966) The Particle Kinetics of Plasmas, Addison-Wesley.

$M$  = atomic weight of target material.

$N_0$  = Avogadro's number.

Shock formation in the ambient gas is described by adding a pseudo-viscous pressure term (QSV) to Eqs. (11), (17), and (23) (Richtmyer and Morton<sup>21</sup>):

In Eq. (17),

$$kN_N T_N \rightarrow kN_N T_N + QSV.$$

In Eq. (23),

$$\Gamma_N T_N \rightarrow (\Gamma_N / N_N)(N_N T_N) + \left(\frac{QSV}{k}\right) (\Gamma_N / N_N),$$

where

$$QSV = 2(\Delta x)^2 (m_N / N_N) \left[ \frac{\partial \Gamma_N}{\partial x} \right]^2.$$

Here,  $\Delta x$  = spatial step size. The addition of the pseudo-viscous pressure QSV allows  $N_N$ ,  $\Gamma_N$ , and  $T_N$  to vary smoothly over a shocked region with a shock-front thickness about equal to several  $\Delta x$ .

It was explained in a previous report<sup>9</sup> that the numerical integration of Eqs. (7), (8), (9), (10), (11), (12), (16), (17), (18), (20), (21), (22), (23), (24), (34), (36), (40), (41), and (45) is greatly facilitated by breaking them down into subgroups. First, the partial differential equations are converted to a set of partially implicit, partially explicit (PI - PE) difference equations.<sup>21</sup> If these equations are properly grouped, then the PI - PE difference equations within each group may be solved independently of the equations in other groups.

The system of PI - PE difference equations may be written in matrix form as

$$\underline{A} \underline{u} = \underline{B}, \quad (47)$$

where  $\underline{u}$  is a column vector representing the unknown dependent variables at the new time step  $t + \Delta t$ ,  $\underline{A}$  is a matrix composed of known transport coefficients at the old time  $t$ , and  $\underline{B}$  is a column vector composed of known dependent variables and transport coefficients at the old time  $t$ . The determination of the dependent variables ( $N_N$ ,  $N_e$ ,  $N_T$ ,  $N_{ex}$ ,  $N_{IT}$ ,  $\Gamma_N$ ,  $\Gamma_e$ , etcetera) at the new time step  $t + \Delta t$  involves the inversion of the matrix  $\underline{A}$ . The determination of  $\underline{A}^{-1}$  is greatly facilitated by grouping the equations as follows:

Group I, ambient gas atoms  $\rightarrow$  Eqs. (11), (17), and (23);

Group II, excited state atoms  $\rightarrow$  Eqs. (8), and (18);



Group III, electrons and ions  $\rightarrow$  Eqs. (7), (10), (20), (21), (34), (36), (40), and (41);

Group IV, target vapor  $\rightarrow$  Eqs. (12), (16), and (22).

By following this particular subdivision into groups, the matrix  $\underline{\underline{A}}$  to be inverted for each subgroup is much smaller than the matrix corresponding to all equations considered simultaneously. This subdivision into groups results in great saving of computer storage requirements and computer running time.

A subroutine called Define has been written to create the appropriate entries in  $\underline{\underline{A}}$  and  $\underline{\underline{B}}$  for each subgroup of equations. Since the original differential equations were of second order in the spatial variable  $x$ , the corresponding difference equations are of second order in the spatial step size  $\Delta x$ . This implies that  $\underline{\underline{A}}$  is a band structured matrix, with many co-diagonals identically zero. The band structure of  $\underline{\underline{A}}$  is decomposed in Define into a single column vector, as described in the IBM scientific subroutine package entitled GELB<sup>34</sup> (Gauss Elimination Band). This scientific subroutine package GELB solves  $M$  simultaneous equations in  $M$  unknowns very efficiently by Gauss elimination with column pivoting only (Hildebrand<sup>35</sup>).

The high energy laser-target interactions computer program consists of a main program that calls about 40 subroutines. The initial conditions for the particle densities, fluxes, and temperatures are read in as data. The value of the initial target temperature is specified, and the value of the incident laser field intensity  $E_{INC}$  is also specified. Parameters determining the degree of implicitness of the difference equations and the spatial step size  $\Delta x$  are initially given.

The electric field  $E_y$  and magnetic field  $H_z$  are determined at each time step from Eqs. (45) and (24).

The step-by-step time integration of these transport equations is accomplished by calling the subroutines Define and Gelb from the main program for each subgroup of equations. This determines all the dependent variables along the new time line  $(t + \Delta t)$ . The time step  $\Delta t$  is automatically adjusted in the main program by requiring that the successive changes in the dependent variables lie between certain preselected tolerances. Let

$$TOL_k = \frac{U_k(t + \Delta t) - U_k(t)}{U_k(t + \Delta t)},$$

where  $U_k$  is any dependent variable (such as  $N_e$ ,  $\Gamma_N$ , and so forth). If  $TOL_k$  for all variables is less than  $TOLMIN$ , the time step  $\Delta t$  is increased by 20 percent.

34. IBM Application Program (1970) System/360 Scientific Subroutine Package, Version III, edition GH20-0205-4.

35. Hildebrand, F.B. (1956) Introduction to Numerical Analysis, McGraw-Hill.

To reduce the truncation error, the time step  $\Delta t$  is cut in half if  $TOL_k$  is greater than TOLMAX for any dependent variable. Also, to increase the efficiency of the program, if  $TOL_k$  is less than 0.1 TOLMIN for a particular subgroup of equations for ten consecutive time steps, then that subgroup of equations is "frozen out" or not integrated, for ninety consecutive time steps. All the transport coefficients such as  $\nu_I$ ,  $\nu_I^{ex}$ ,  $\nu_{IT}$ ,  $\nu_{ex}$ ,  $\alpha_r$ ,  $\nu_{eN}$ , and so forth, are evaluated at each time step in separate computer subroutines.

The computer output consists of listings of all the dependent variables as a function of position at each time step. Also, the laser field intensity at the target surface and the target surface temperature are given at each time step.

### 3. CONCLUSIONS

It was explained in reference 9 how the high energy laser-target interactions program was checked out. Let

P = degree of implicitness for first order spatial derivatives,

S = degree of implicitness for second order spatial derivatives,

Z = relative fraction taken for forward differences along the new time line,

V = relative fraction taken for forward differences along the old time line.

For example,  $S = 0$  corresponds to a fully explicit integration scheme for second order spatial derivatives and  $S = 1$  corresponds to a fully implicit scheme. Also,  $Z = 1$  corresponds to taking forward differences along the new time line, and  $Z = 0$  corresponds to taking backward differences along the new time line.

In this report, the spatial step size  $\Delta x$  is nonuniform. The step size  $\Delta x$  was taken equal to  $2.676 \times 10^{-7}$  meters at the target surface. Each succeeding step size is increased 3.5 percent as one recedes away from the target surface. The maximum number of incremental steps equals 154. The total distance considered equals 1.521 mm. Maximum numerical stability was achieved with the following scheme:

$S = 0.5$	} For Group I (neutral atoms), Group II (excited state atoms), Group IV (target vapor).
$P = 0.5$	

$S = 1.0$	} For Group III (electrons and ions).
$P = 1.0$	

Let J represent an index to count the position of the step size  $\Delta x$ , so that  $J = 1$  corresponds to the target surface and  $J = 155$  corresponds to the position of the incident laser beam. The parameters V and Z are chosen so that

$$V = 0.5 ,$$

$$Z = 0.5 .$$

This corresponds to taking central differences.

In this report, the laser frequency  $\omega$  is set equal to  $1.77826 \times 10^{14}$  rad/sec (CO<sub>2</sub> laser frequency). The target is aluminum and the ambient gas is xenon. In the figures, the initial conditions on the variables  $\Gamma_N$ ,  $N_N$ ,  $T_N$ ,  $\Gamma_{ex}$ ,  $N_{ex}$ ,  $T_I$ ,  $T_e$ ,  $N_e$ ,  $N_{IT}$ ,  $N_T$ , and  $T_T$  are obtained by first selecting reasonable profiles for these variables and then letting the program run with a small value for  $E_{INC}$  (incident field intensity) until the successive changes in the variables become relatively small. Each case is illustrated by a set of two figures; one figure represents the particle densities as a function of position at a given instant in time and another figure represents the particle temperatures as a function of position at a given instant in time. In these figures,

- → electrons,
- → neutral gas atoms,
- ◇ → target vapor atoms,
- △ → in the density plots, excited state atoms,
- △ → in the temperature plots, ion temperature.

The distance  $x$  is normalized in these plots:  $x/L$ , where  $L$  = total laser path length = 1.521 mm.

In Figures 1 and 2,  $E_{INC}$  is set equal to 1 volt/meter ( $2.7 \times 10^{-7}$  watts/cm<sup>2</sup>) and it may be noted that, after an elapsed time of 0.257  $\mu$ sec, all density and temperature profiles are fairly uniform in space. The final density and temperature profiles in Figures 1 and 2 are used as initial conditions in all subsequent calculations. In this report, the incident field  $E_{INC}$  starts from a very low value (1 volt/meter) and rises as the square root of the elapsed time. This implies that the incident flux rises linearly with time, and the rise time is adjusted so that the incident flux reaches its peak value after an elapsed time of 0.1  $\mu$ sec.

In Figures 3 and 4,  $E_{INC} = 6 \times 10^6$  volts/meter ( $0.95 \times 10^7$  watts/cm<sup>2</sup>), and the elapsed time = 0.618  $\mu$ sec. Ionization due to a neutral atom (ambient gas or target vapor) colliding with a target vapor atom is neglected ( $\nu_{NNIT} = 0$ ). The heat diffusion in the target vapor away from the target surface may be noted in Figure 4. In Figures 5 and 6,  $E_{INC} = 6 \times 10^6$  V/m, and the elapsed time = 1.41  $\mu$ sec. Also,  $\nu_{NNIT} = 0$ . Comparing Figure 6 with Figure 4, it may be noted that the diffusion of heat away from the target surface continues in the target vapor. However, it may be noted that there is no initiation of a laser absorption wave (LAW) at this incident power density ( $0.95 \times 10^7$  watts/cm<sup>2</sup>).

In Figures 7 and 8,  $E_{\text{INC}} = 2 \times 10^7 \text{ V/m}$  ( $1.06 \times 10^8 \text{ watts/cm}^2$ ) and the elapsed time =  $0.048 \mu\text{sec}$ . The ionization due to a neutral atom colliding with a target vapor atom is neglected ( $\nu_{\text{NNIT}} = 0$ ). In Figures 9 and 10, the conditions are the same as in Figures 7 and 8, except that the elapsed time =  $0.103 \mu\text{sec}$ . It may be observed that the electron density is increasing at a distance of about one wavelength from the target surface. This indicates the ignition of a LAW. In Figure 10, it may be observed that the ambient gas temperature reaches a peak value of about  $10^4 \text{ }^\circ\text{K}$ , near the target surface. Also, the target vapor temperature reaches a peak value of about  $10^6 \text{ }^\circ\text{K}$  near the target surface. This is physically unrealistic, because at this temperature two target vapor atoms would collide and ionize. This shows that target vapor atom-target vapor atom impact ionization may not be neglected in the ignition of LAW's ( $\nu_{\text{NNIT}} \neq 0$ ). The target vapor reaches a high temperature because the target vapor atoms are being rapidly emitted from the surface and are diffusing into approximately one atmosphere of xenon gas, so that the target vapor is undergoing rapid, nearly adiabatic compression. The target vapor hasn't been able to transfer all of its excess energy to the xenon gas on this time scale ( $0.103 \mu\text{sec}$ ).

In Figures 11 through 18,  $E_{\text{INC}} = 6 \times 10^6 \text{ V/m}$  ( $0.95 \times 10^7 \text{ watts/cm}^2$ ). Also, target vapor atom-target vapor atom impact ionization is not neglected ( $\nu_{\text{NNIT}} \neq 0$ ). Comparing Figures 3 through 6 with Figures 11 through 18 ( $E_{\text{INC}} = 6 \times 10^6 \text{ V/m}$  in all these figures), it may be noted that the densities and temperatures are about the same when  $\nu_{\text{NNIT}} = 0$  and  $\nu_{\text{NNIT}} \neq 0$  for comparable elapsed times. Also, for the case when  $\nu_{\text{NNIT}} \neq 0$ , it may be noted that there is no ignition of LAW's at  $E_{\text{INC}} = 6 \times 10^6 \text{ V/m}$ .

In Figures 19 through 24,  $E_{\text{INC}} = 2 \times 10^7 \text{ V/m}$  ( $1.06 \times 10^8 \text{ watts/cm}^2$ ). Target vapor atom-target vapor atom impact ionization is not neglected ( $\nu_{\text{NNIT}} \neq 0$ ). The elapsed time in Figure 23 ( $0.074 \mu\text{sec}$ ) is roughly comparable with the elapsed time in Figure 9 ( $0.103 \mu\text{sec}$ ). However, the peak target vapor density in Figure 23 is about one order of magnitude less than in Figure 9. Also, it may be seen that the peak target vapor temperature is almost an order of magnitude less in Figure 24 compared with Figure 10. One may discern from Figure 23 the ignition of a LAW by an increase in the electron density profile at a distance of about two laser wavelengths from the aluminum target surface.

In Figures 25 through 28,  $E_{\text{INC}} = 2 \times 10^7 \text{ V/m}$  and  $\nu_{\text{NNIT}} \neq 0$ , just as in Figures 19 through 24, except that in Figures 25 through 28, the diffusion of the electrons and ambient gas ions is uncoupled from the diffusion of the target vapor ions. This uncoupling is achieved by letting  $\text{DIFFE2} \rightarrow 0$  in Eqs. (40),  $\text{DIFFI2} \rightarrow 0$  and  $\text{ANLPI} \rightarrow 0$  in Eq. (41), and  $(N_{\text{IT}}/N_e) \rightarrow 0$  in the expressions for  $\text{DIFFE1}$  and  $\text{DEN}$  under Eq. (41). Comparing Figures 25 and 26 with Figures 19 and 20, and Figures 27 and 28 with Figures 23 and 24, it may be observed that this uncoupling procedure produces no discernible effects in the density or temperature profiles for comparable elapsed times.

In Figures 29 through 38,  $E_{\text{INC}} = 2 \times 10^7 \text{ V/m}$  ( $1.06 \times 10^8 \text{ watts/cm}^2$ ) and  $v_{\text{NNIT}} \neq 0$ . The tic marks in the density and temperature profiles at  $x = 0.9L$  indicate a scale change in Figures 29 through 38. In Figures 29 and 30, the elapsed time =  $0.079 \mu\text{sec}$ . The ignition of a LAW may be clearly observed in Figure 29 by the increase in the electron density profile at a distance of about  $10^{-5}$  meters (one laser wavelength) from the target surface. In Figure 29, it may be seen that the aluminum vapor layer extends from  $x = 0.94L$  up to  $x = L$ .

In Figure 30, it may be noted that the target vapor temperature reaches a value of about  $2 \times 10^6 \text{ K}$  at the outer edge of the aluminum vapor layer ( $x = 0.94L$ ), due to nearly adiabatic compression. The vapor emerging at the target surface is about  $2000^\circ\text{K}$ .

From Figure 29, it is seen that the target vapor density  $N_T$  increases as  $x$  increases towards the target surface ( $x = L$ ). Also, from Figure 30 it is seen that the target vapor temperature  $T_T$  increases rapidly as the edge of the vapor layer is reached, and then decreases more slowly as  $x$  approaches the target surface. Since the rate of production of electrons by the process  $\text{Al} + \text{Al} \rightarrow \text{Al} + \text{Al}^+ + e$  increases as  $N_T$  and  $T_T$  increase, it is not surprising that the electron density buildup shown in Figure 29 occurs somewhere in the middle of the vapor layer extending from  $x = 0.94L$  to  $x = L$ . Figures 31 through 38 show the further development of the laser absorption wave. In Figure 35 (elapsed time =  $0.1 \mu\text{sec}$ ) and in Figure 37 (elapsed time =  $0.102 \mu\text{sec}$ ), the target vapor density exceeds the xenon gas density. Also, from Figures 36 and 38 it may be seen that close to the target surface the xenon gas temperature  $T_N$  has increased to over  $2000^\circ\text{K}$ , having been heated primarily through elastic collisions with the aluminum vapor atoms. Now, the xenon gas is sufficiently hot so that the process  $\text{Xe} + \text{Xe} \rightarrow \text{Xe} + \text{Xe}^+ + e$  also plays a role in the electron density buildup. This process accounts for the "spike" on the electron density profile near the target surface that occurs in Figures 35 and 37.

To summarize, the early stages in the ignition of a LAW from an aluminum target in xenon were observed at a power density of  $10^8 \text{ watts/cm}^2$ . Starting with a low density of "priming" electrons of  $10^6/\text{cm}^3$  (due to "prompt" field emission in time scales less than or of the order of 1 nsec), the first mechanism responsible for substantial electron density buildup is  $\text{Al} + \text{Al} \rightarrow \text{Al} + \text{Al}^+ + e$ . Later, as the ambient xenon gas is heated by the hot target vapor through elastic collisions, a second electron density buildup mechanism starts to play a role:



Shock waves can be generated in the ambient gas, but not in the electron gas, since  $v_x^e$  is always much less than  $\sqrt{3kT_e/m}$ . Also, there is considerable

difference between the temperatures of the electrons, ions, target vapor atoms, and xenon gas atoms. The computer program that has been developed can be used to study the further development of LAW's. Also the ignition and propagation of LAW's from various materials (such as dielectrics, or coated metal targets) may be investigated.

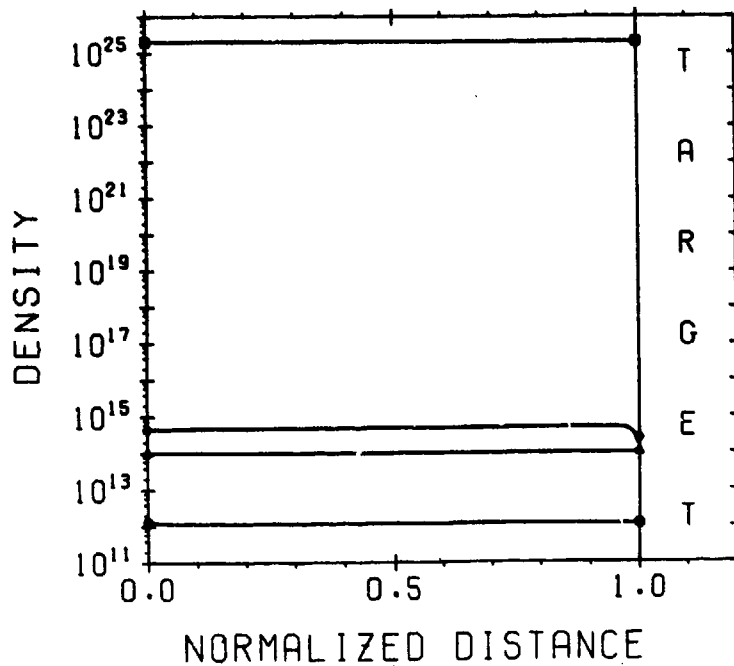


Figure 1. Particle Density vs Normalized Distance  
( $E = 0$  MV/m; Time =  $0.257 \times 10^{-6}$  sec)

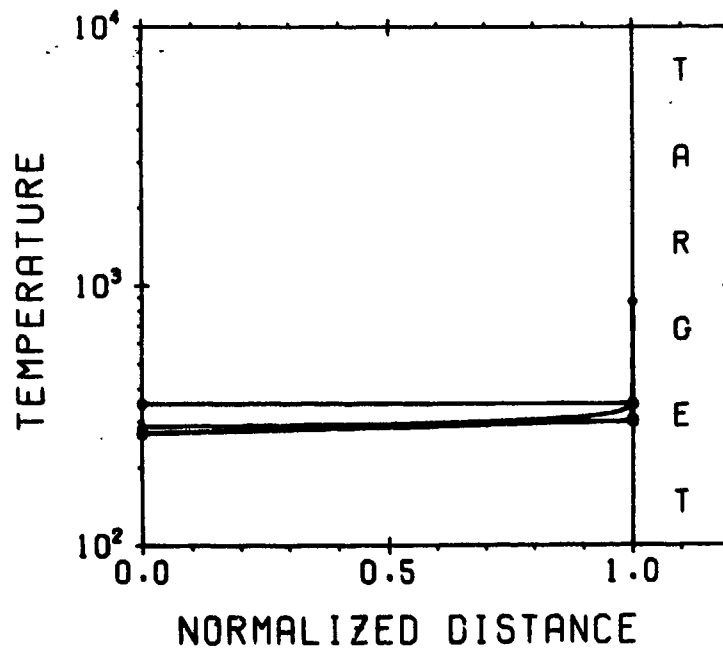


Figure 2. Temperature ( $^{\circ}$ K) vs Normalized Distance  
( $E = 0$  MV/m; Time =  $0.257 \times 10^{-6}$  sec)

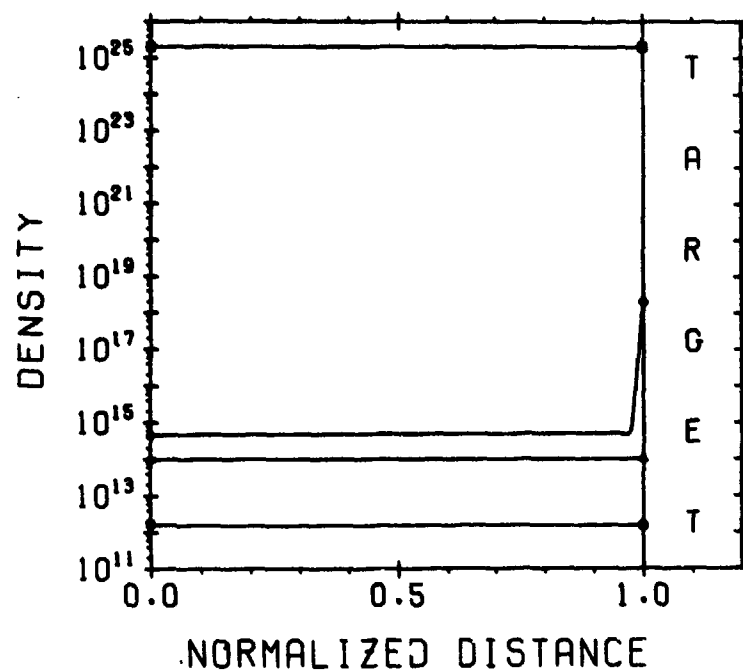


Figure 3. Particle Density vs Normalized Distance  
( $E = 6 \text{ MV/m}$ ; Time =  $0.618 \times 10^{-6} \text{ sec}$ )

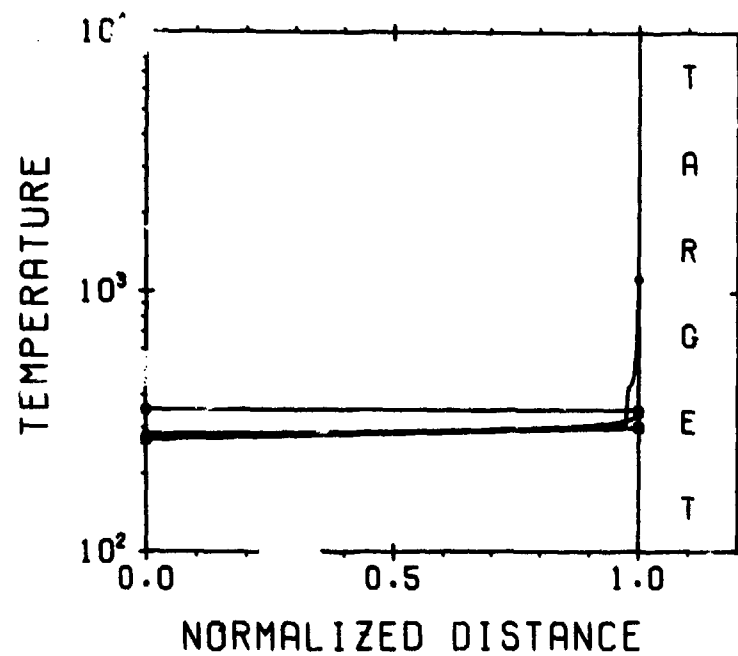


Figure 4. Temperature ( $^{\circ}\text{K}$ ) vs Normalized Distance  
( $E = 6 \text{ MV/m}$ ; Time =  $0.618 \times 10^{-6} \text{ sec}$ )



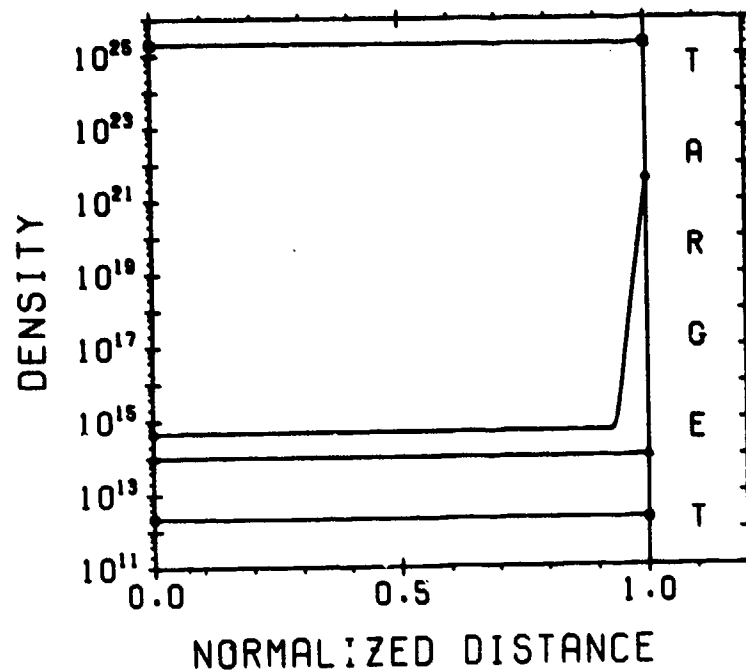


Figure 5. Particle Density vs Normalized Distance  
( $E = 6 \text{ MV/m}$ ; Time =  $1.411 \times 10^{-6} \text{ sec}$ )

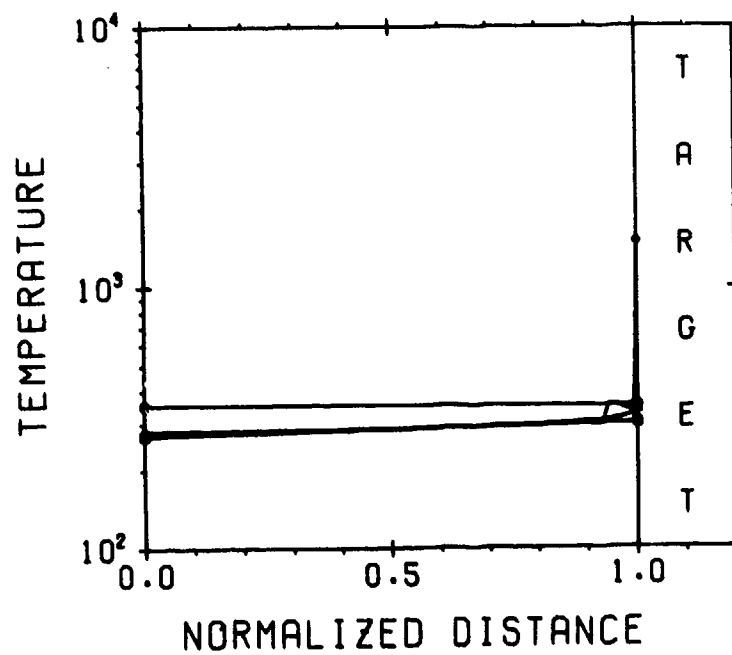


Figure 6. Temperature ( $^{\circ}\text{K}$ ) vs Normalized Distance  
( $E = 6 \text{ MV/m}$ ; Time =  $1.411 \times 10^{-6} \text{ sec}$ )

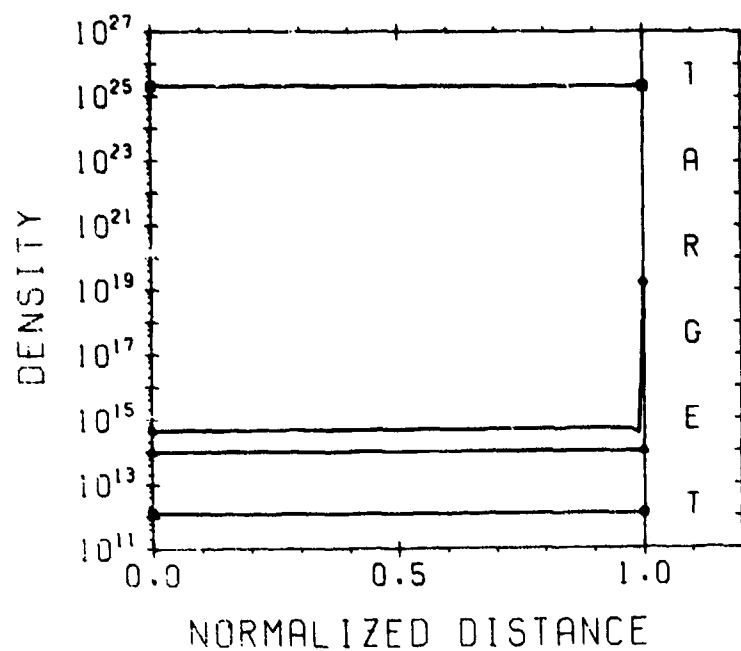


Figure 7. Particle Density vs Normalized Distance  
( $E = 20 \text{ MV/m}$ ; Time =  $0.048 \times 10^{-6} \text{ sec}$ )

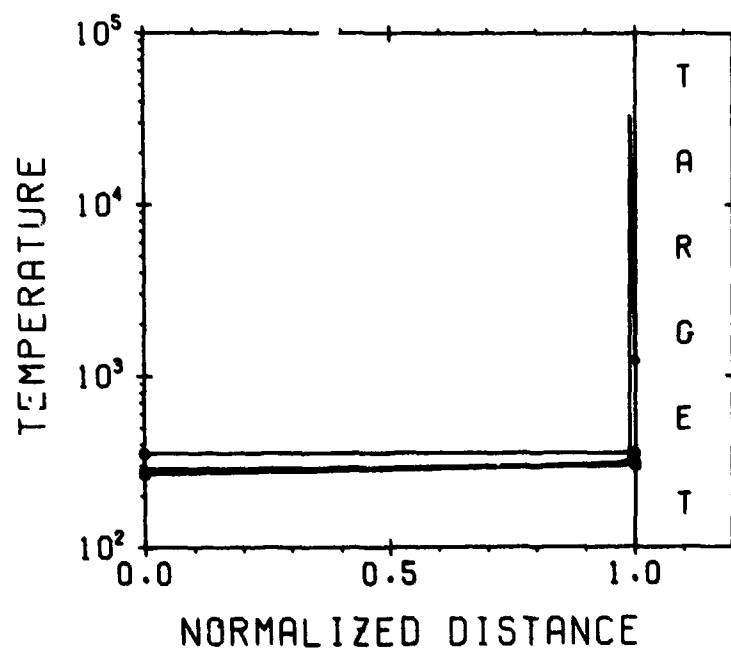


Figure 8. Temperature ( $^{\circ}\text{K}$ ) vs Normalized Distance  
( $E = 20 \text{ MV/m}$ ; Time =  $0.048 \times 10^{-6} \text{ sec}$ )

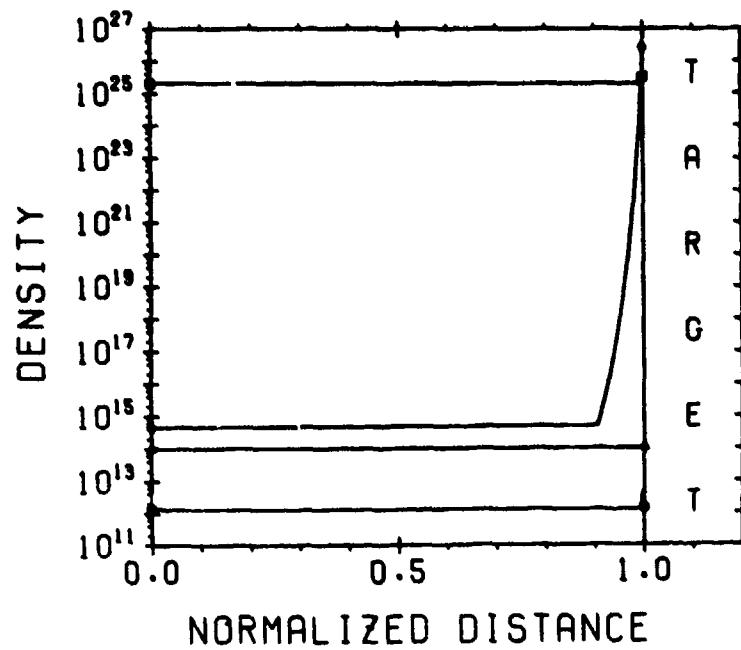


Figure 9. Particle Density vs Normalized Distance  
( $E = 20$  MV/m; Time =  $0.103 \times 10^{-6}$  sec)

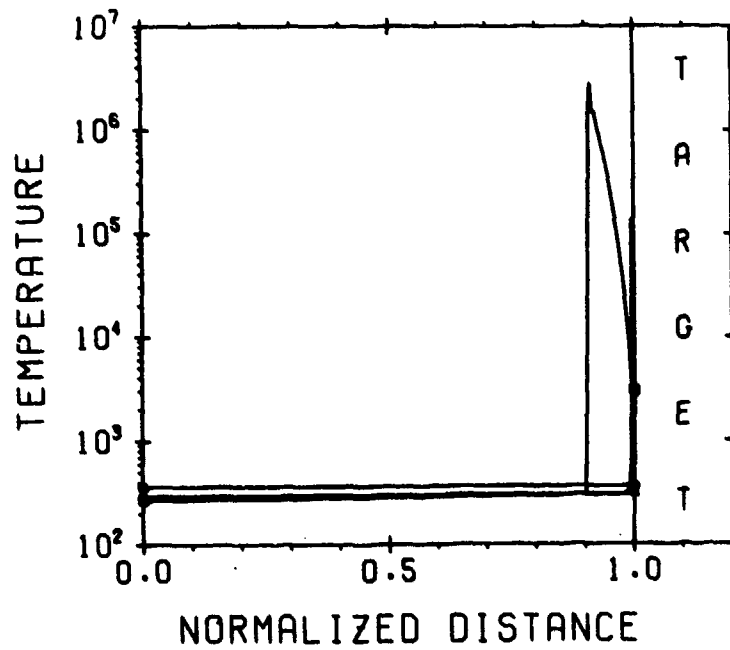


Figure 10. Temperature ( $^{\circ}\text{K}$ ) vs Normalized Distance  
( $E = 20$  MV/m; Time =  $0.103 \times 10^{-6}$  sec)

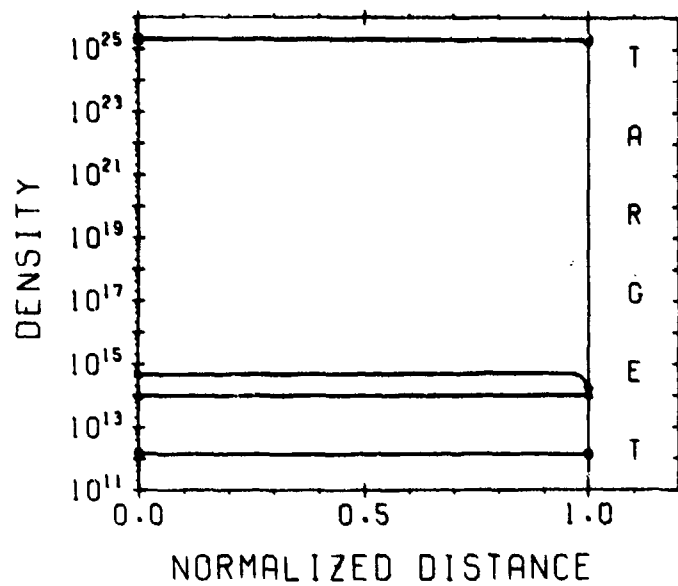


Figure 11. Particle Density vs Normalized Distance  
( $E = 6 \text{ MV/m}$ ; Time =  $0.248 \times 10^{-6} \text{ sec}$ )

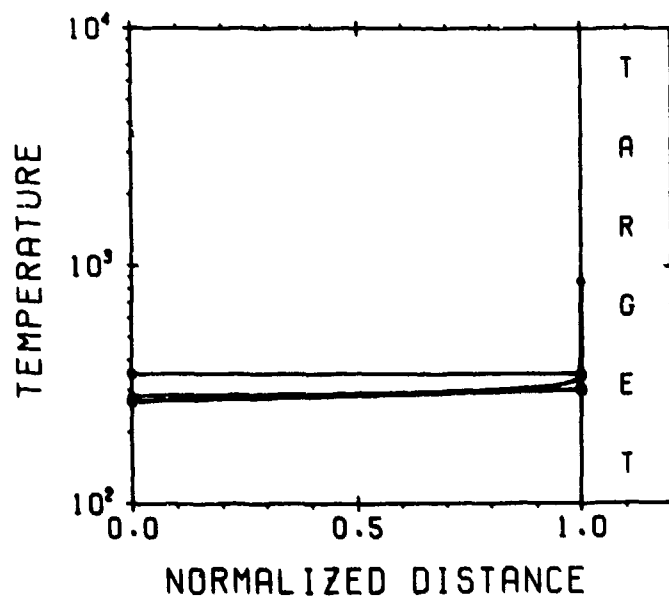


Figure 12. Temperature ( $^{\circ}\text{K}$ ) vs Normalized Distance  
( $E = 6 \text{ MV/m}$ ; Time =  $0.248 \times 10^{-6} \text{ sec}$ )

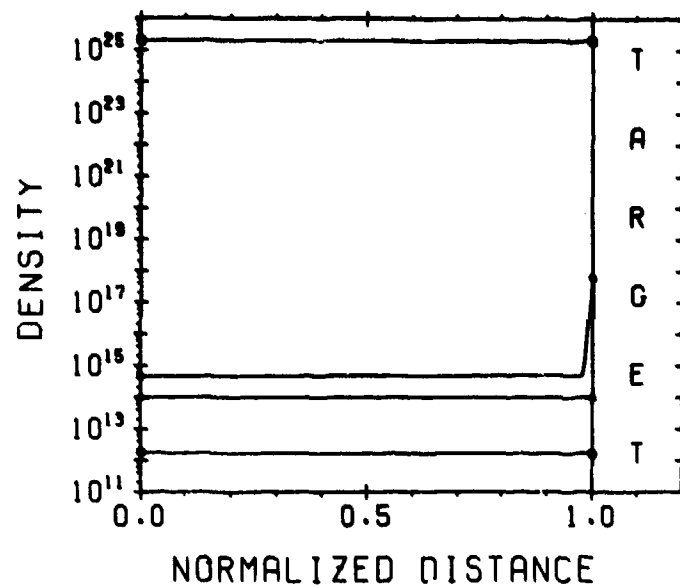


Figure 13. Particle Density vs Normalized Distance  
( $E = 6 \text{ MV/m}$ ; Time =  $0.549 \times 10^{-6} \text{ sec}$ )

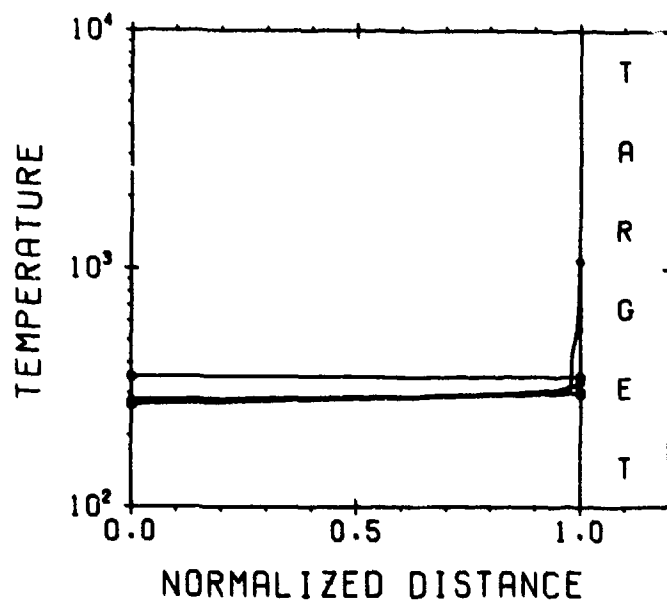


Figure 14. Temperature ( $^{\circ}\text{K}$ ) vs Normalized Distance  
( $E = 6 \text{ MV/m}$ ; Time =  $0.549 \times 10^{-6} \text{ sec}$ )

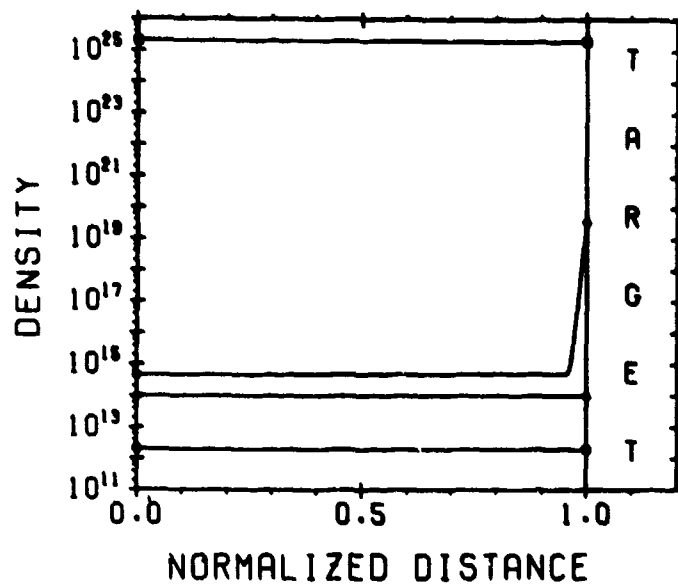


Figure 15. Particle Density vs Normalized Distance  
( $E = 6 \text{ MV/m}$ ; Time =  $0.832 \times 10^{-6} \text{ sec}$ )

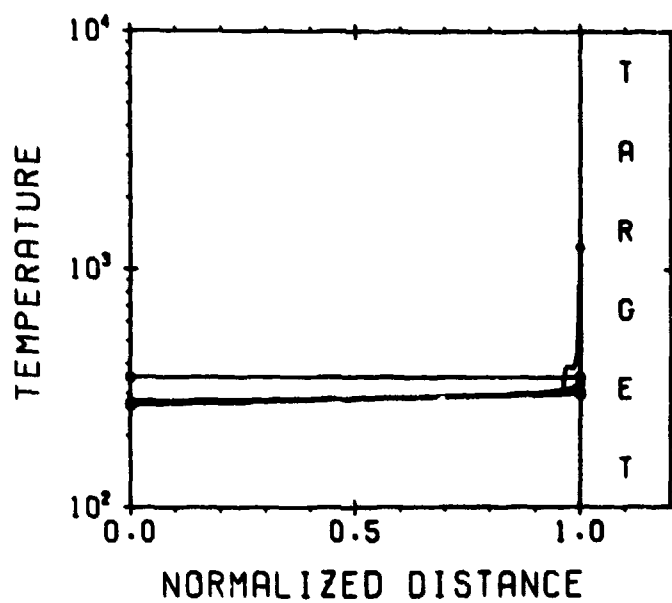


Figure 16. Temperature ( $^{\circ}\text{K}$ ) vs Normalized Distance  
( $E = 6 \text{ MV/m}$ ; Time =  $0.832 \times 10^{-6} \text{ sec}$ )

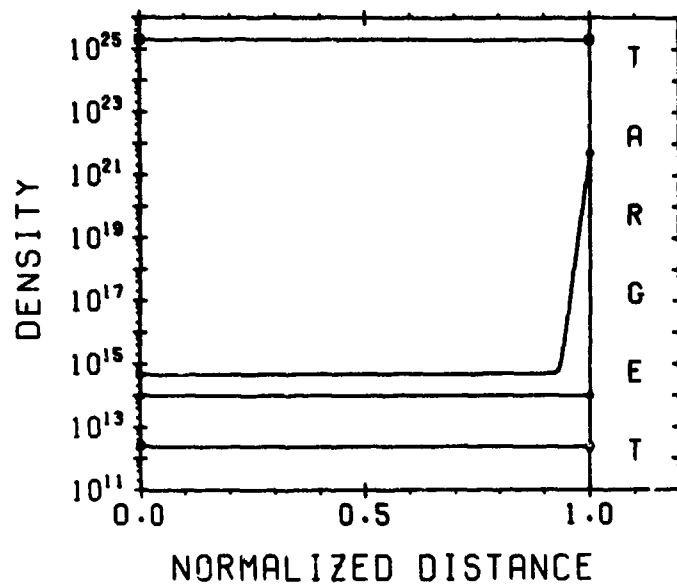


Figure 17. Particle Density vs Normalized Distance  
( $E = 6 \text{ MV/m}$ ; Time =  $1.457 \times 10^{-6} \text{ sec}$ )

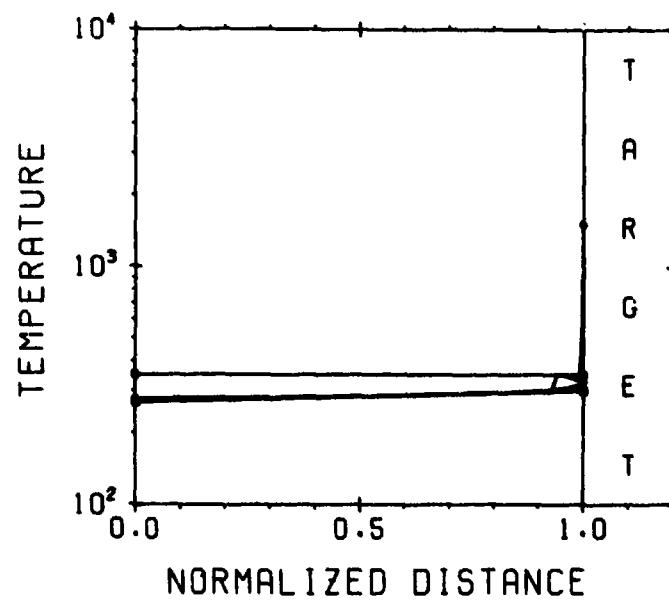


Figure 18. Temperature ( $^{\circ}\text{K}$ ) vs Normalized Distance  
( $E = 6 \text{ MV/m}$ ; Time =  $1.457 \times 10^{-6} \text{ sec}$ )

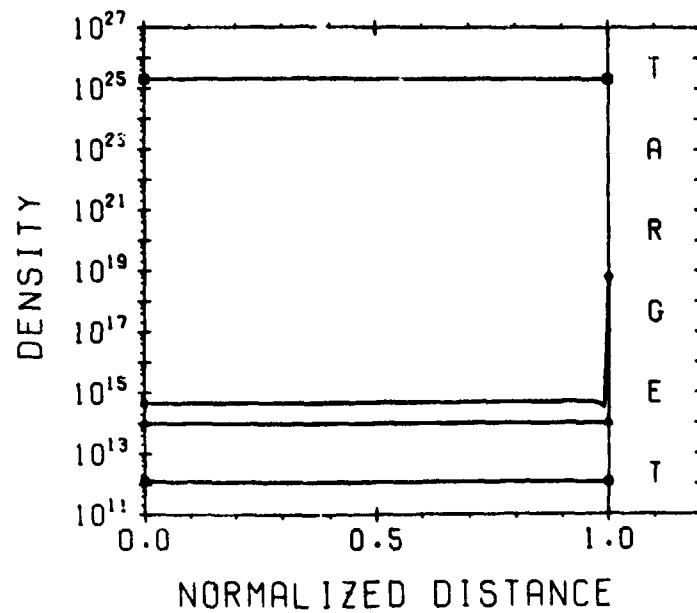


Figure 19. Particle Density vs Normalized Distance  
( $E = 20$  MV/m; Time =  $0.046 \times 10^{-6}$  sec)

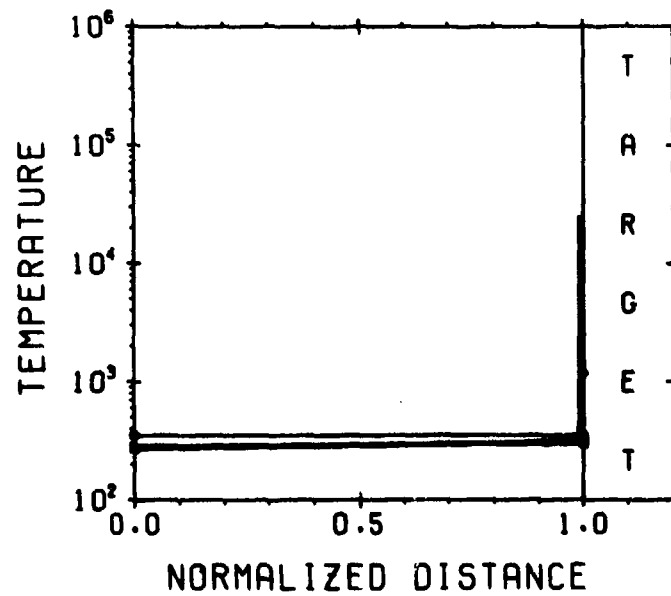


Figure 20. Temperature ( $^{\circ}\text{K}$ ) vs Normalized Distance  
( $E = 20$  MV/m; Time =  $0.046 \times 10^{-6}$  sec)



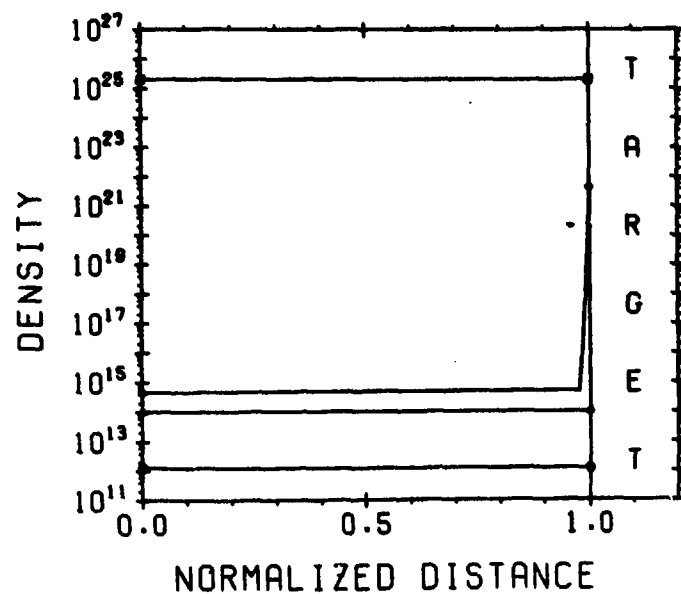


Figure 21. Particle Density vs Normalized Distance  
( $E = 20 \text{ MV/m}$ ; Time =  $0.061 \times 10^{-6} \text{ sec}$ )

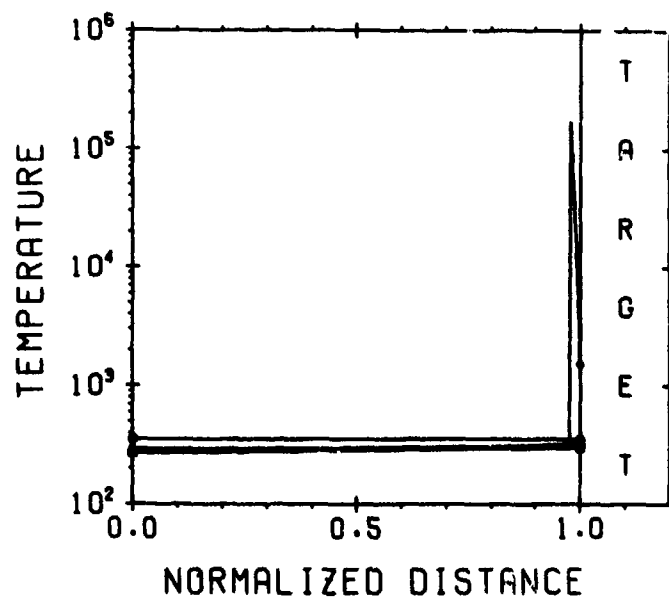


Figure 22. Temperature ( $^{\circ}\text{K}$ ) vs Normalized Distance  
( $E = 20 \text{ MV/m}$ ; Time =  $0.061 \times 10^{-6} \text{ sec}$ )

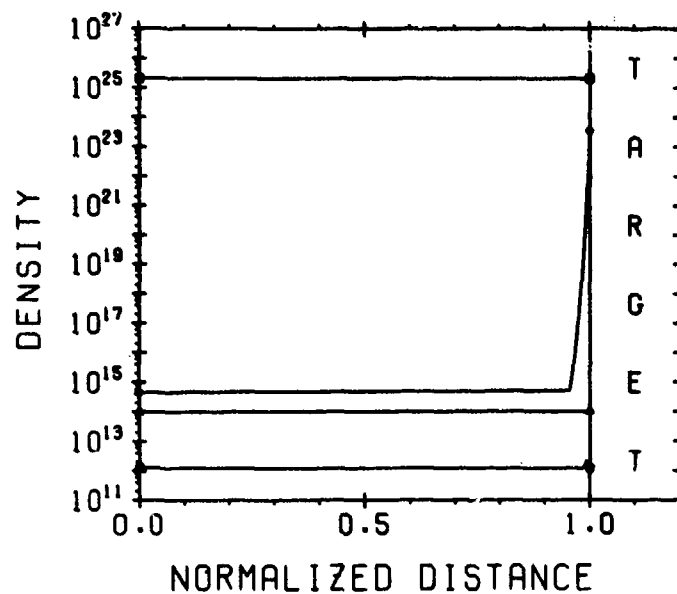


Figure 23. Particle Density vs Normalized Distance  
( $E = 20$  MV/m; Time =  $0.074 \times 10^{-6}$  sec)

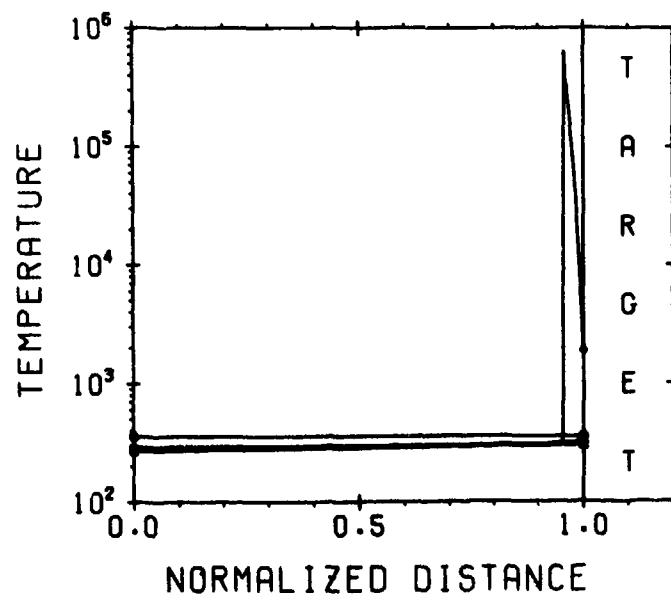


Figure 24. Temperature ( $^{\circ}\text{K}$ ) vs Normalized Distance  
( $E = 20$  MV/m; Time =  $0.074 \times 10^{-6}$  sec)

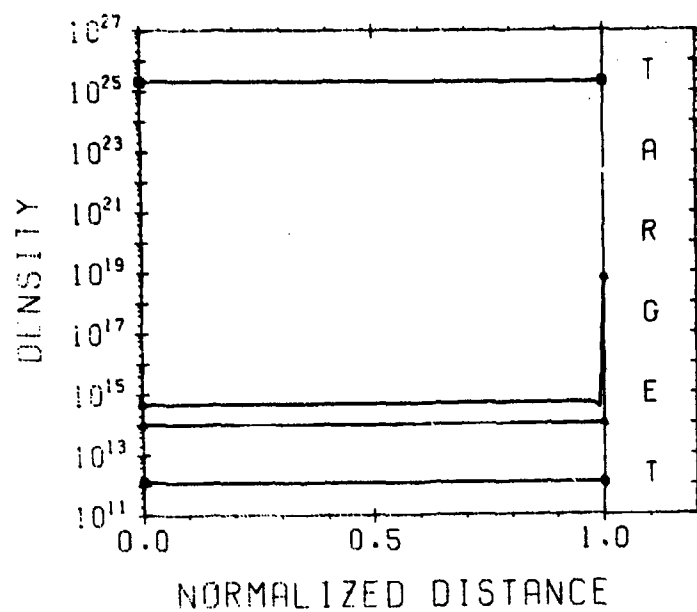


Figure 25. Particle Density vs Normalized Distance  
( $E = 20$  MV/m; Time  $0.046 \times 10^{-8}$  sec; uncoupled diffusion)

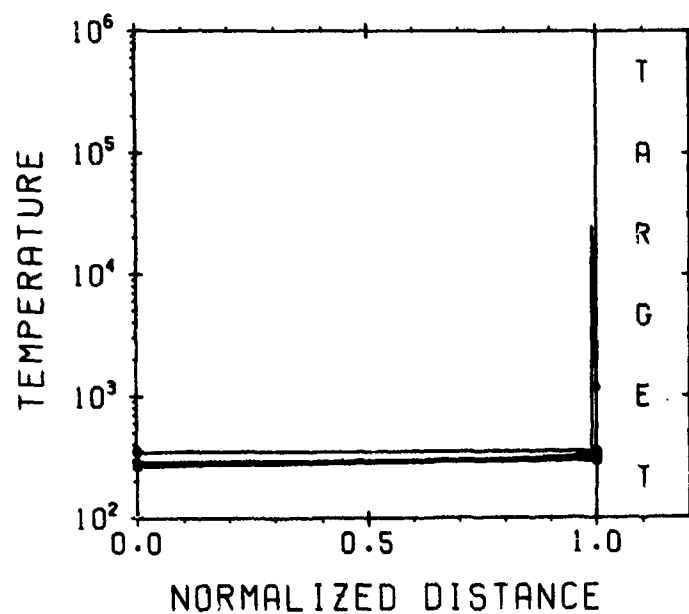


Figure 26. Temperature ( $^{\circ}$ K) vs Normalized Distance  
( $E = 20$  MV/m; Time  $= 0.046 \times 10^{-8}$  sec; uncoupled diffusion)

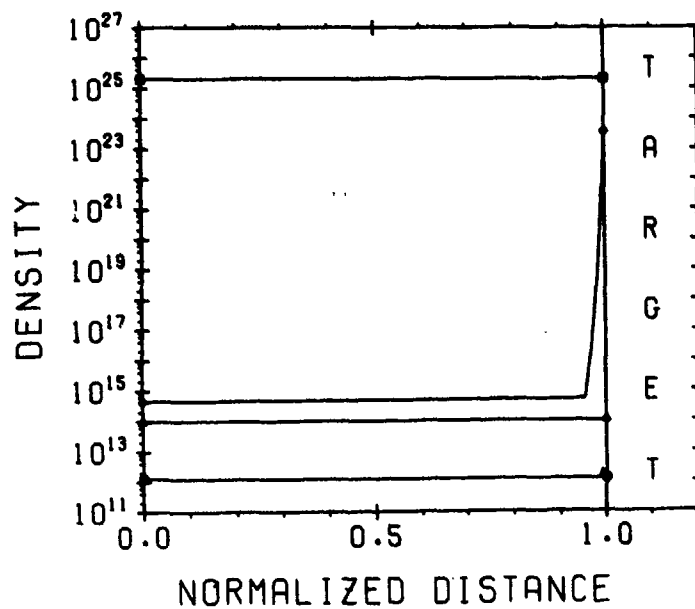


Figure 27. Particle Density vs Normalized Distance  
( $E = 20 \text{ MV/m}$ ; Time =  $0.074 \times 10^{-8} \text{ sec}$ ; uncoupled diffusion)

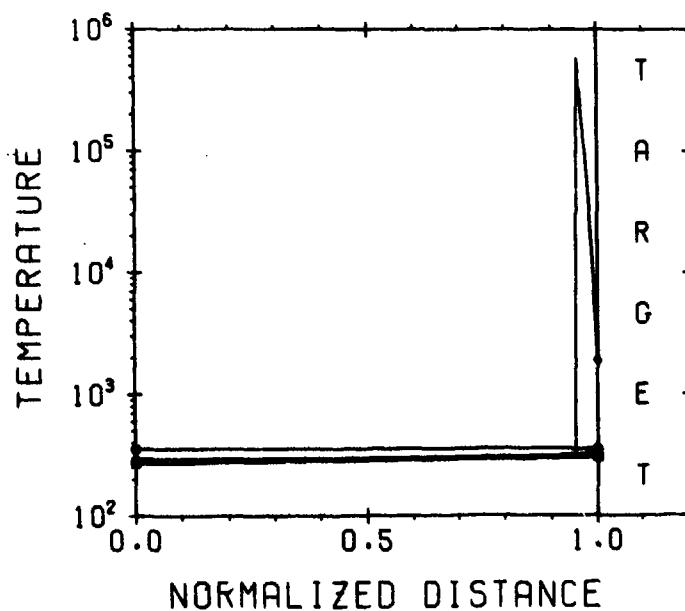


Figure 28. Temperature ( $^{\circ}\text{K}$ ) vs Normalized Distance  
( $E = 20 \text{ MV/m}$ ; Time =  $0.074 \times 10^{-8} \text{ sec}$ ; uncoupled diffusion)

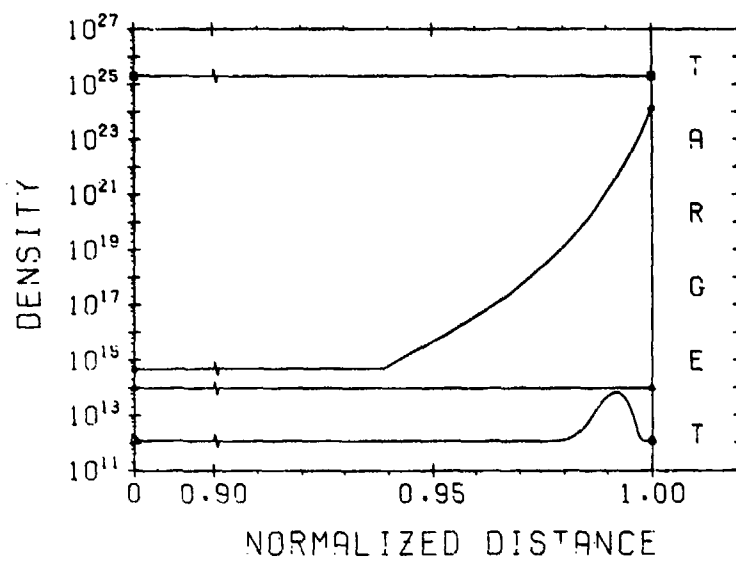


Figure 29. Particle Density vs Normalized Distance  
( $E = 20 \text{ MV/m}$ ; Time =  $0.079 \times 10^{-6} \text{ sec}$ )

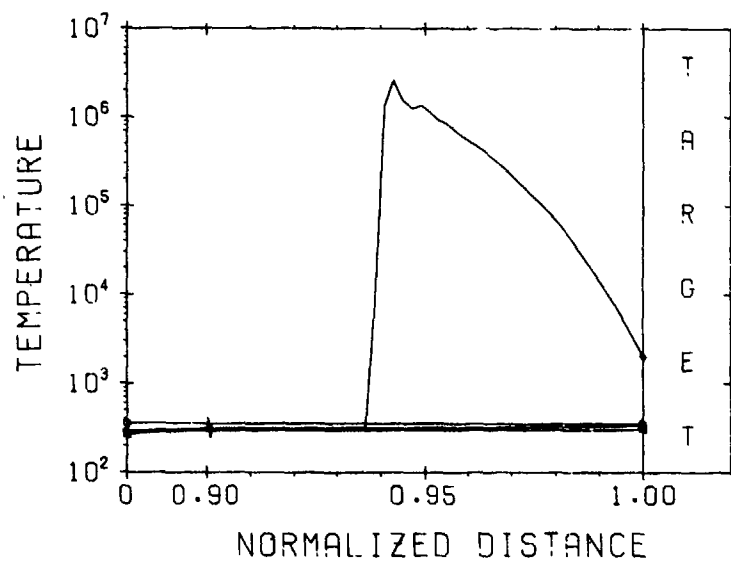


Figure 30. Temperature ( $^{\circ}\text{K}$ ) vs Normalized Distance  
( $E = 20 \text{ MV/m}$ ; Time =  $0.079 \times 10^{-6} \text{ sec}$ )

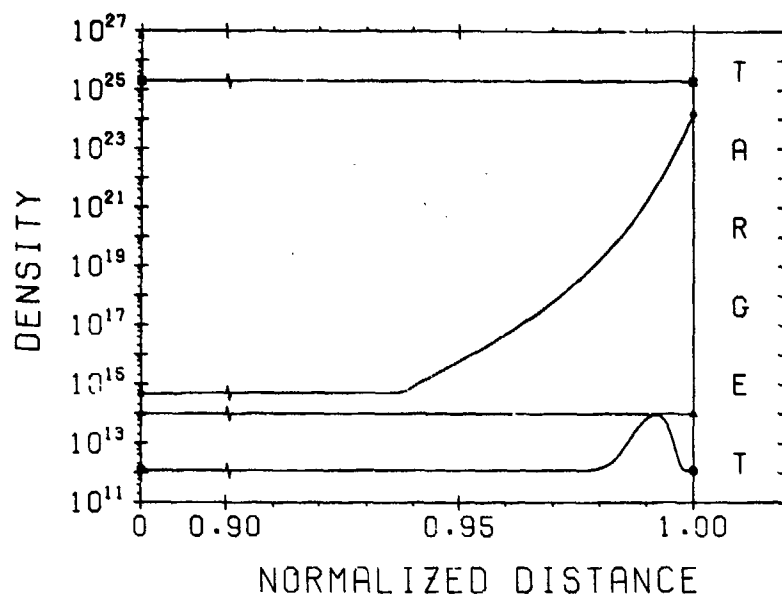


Figure 31. Particle Density vs Normalized Distance  
( $E = 20$  MV/m; Time =  $0.080 \times 10^{-6}$  sec)

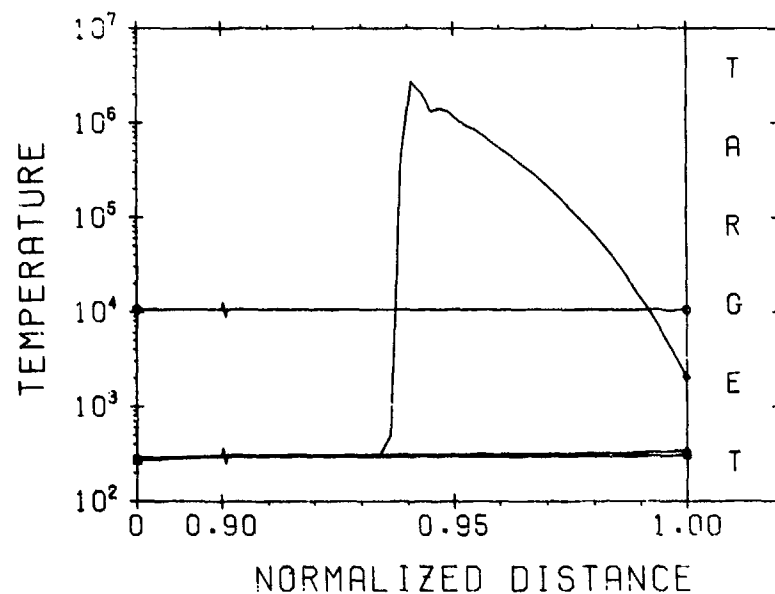


Figure 32. Temperature ( $^{\circ}\text{K}$ ) vs Normalized Distance  
( $E = 20$  MV/m; Time =  $0.080 \times 10^{-6}$  sec)

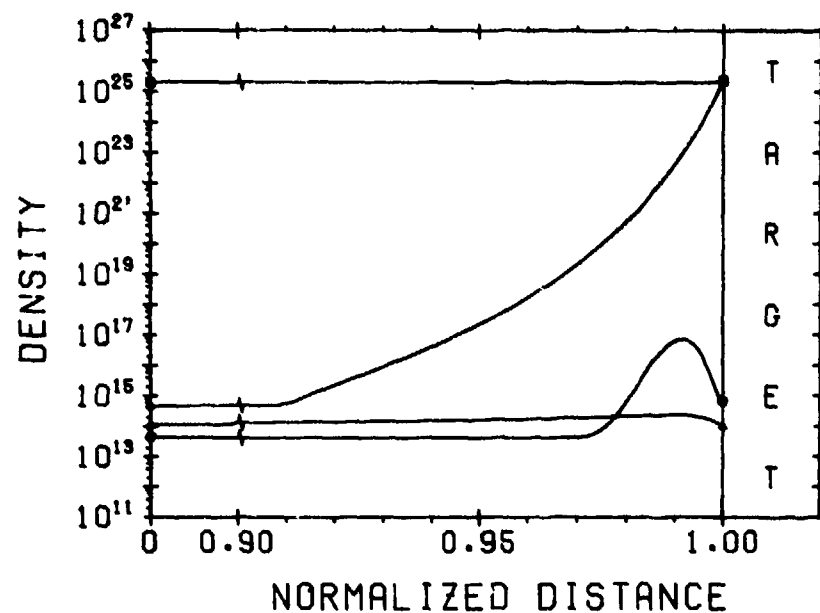


Figure 33. Particle Density vs Normalized Distance  
( $E = 20$  MV/m; Time =  $0.093 \times 10^{-6}$  sec)

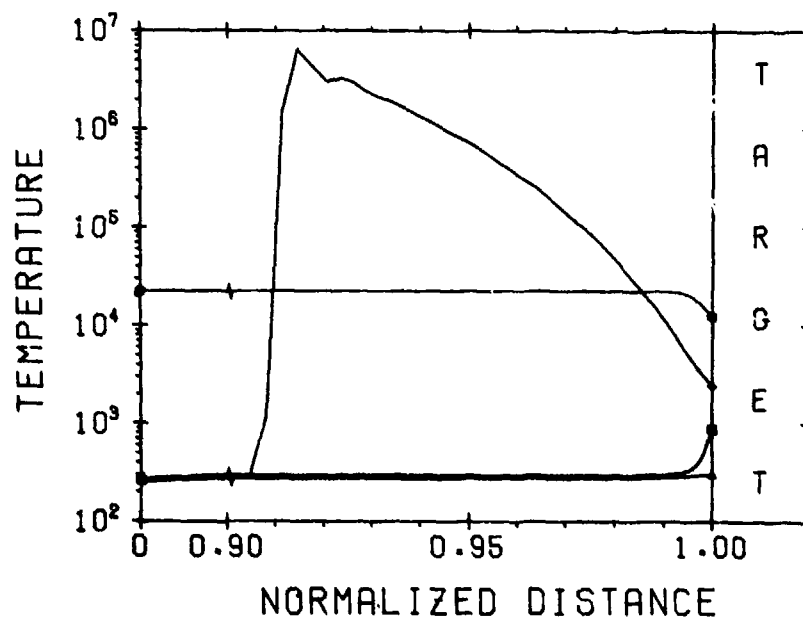


Figure 34. Temperature ( $^{\circ}$ K) vs Normalized Distance  
( $E = 20$  MV/m; Time =  $0.093 \times 10^{-6}$  sec)

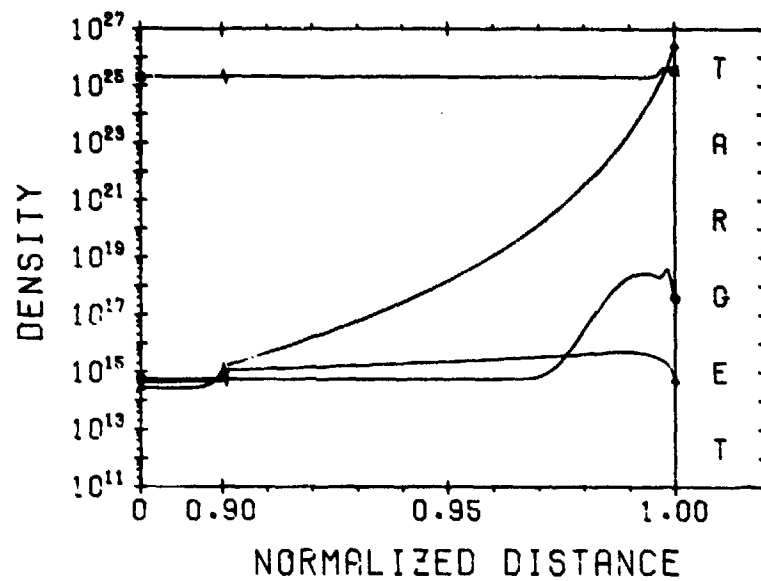


Figure 35. Particle Density vs Normalized Distance  
( $E = 20 \text{ MV/m}$ ; Time =  $0.100 \times 10^{-6} \text{ sec}$ )

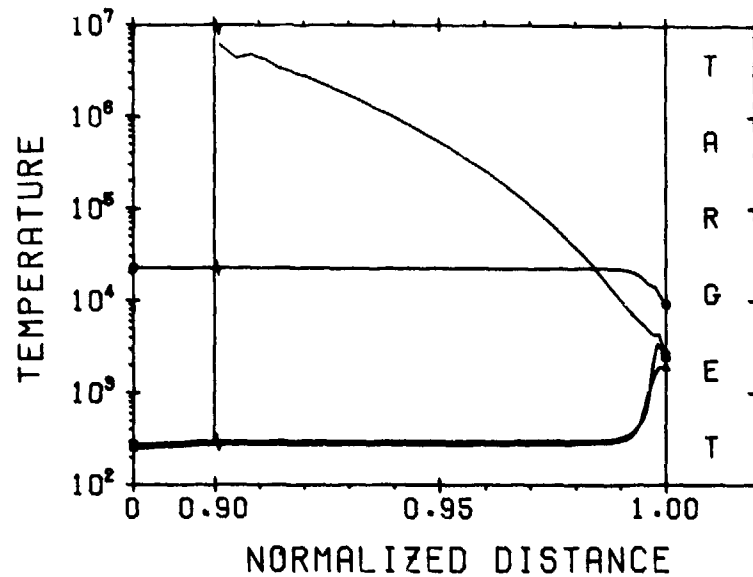


Figure 36. Temperature ( $^{\circ}\text{K}$ ) vs Normalized Distance  
( $E = 20 \text{ MV/m}$ ; Time =  $0.100 \times 10^{-6} \text{ sec}$ )



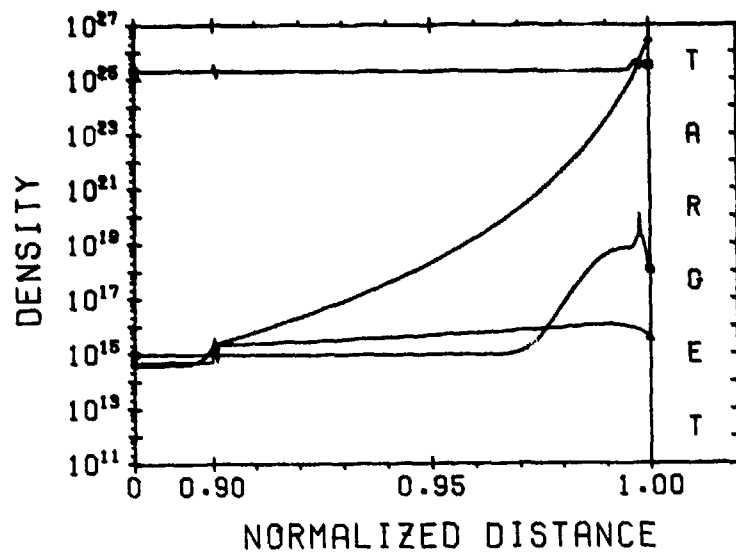


Figure 37. Particle Density vs Normalized Distance  
( $E = 20 \text{ MV/m}$ ; Time =  $0.102 \times 10^{-6} \text{ sec}$ )

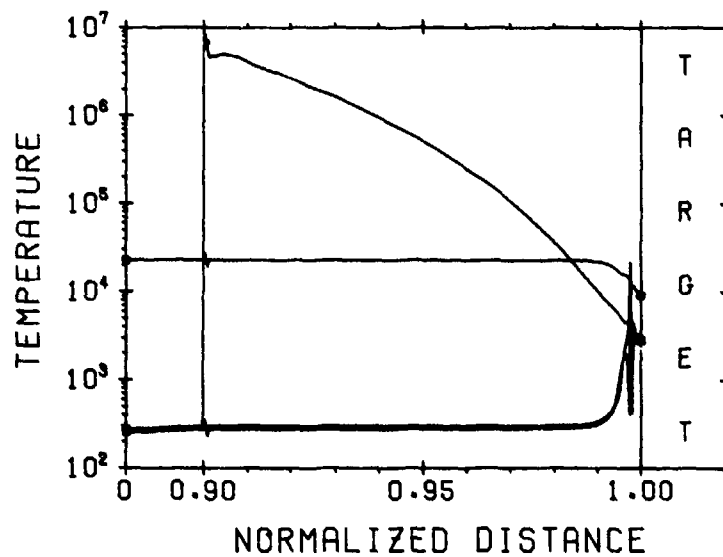


Figure 38. Temperature ( $^{\circ}\text{K}$ ) vs Normalized Distance  
( $E = 20 \text{ MV/m}$ ; Time =  $0.102 \times 10^{-6} \text{ sec}$ )

## References

1. Ready, J. F. (1971) Effects of High-Power Laser Radiation, Academic Press.
2. DeMichelis, C. (1969) IEEE J. Quant. Electronics QE-5:188.
3. DeMichelis, C. (1970) IEEE J. Quant. Electronics QE-6:630.
4. Nielsen, P. E. (1974) Breakdown and laser absorption waves, Jour. Defense Research, Series B, December.
5. Nielsen, P. E. and Canavan, G. H. (1974) Theory of laser target interaction, Jour. Defense Research, Series B, December.
6. Harmon, N. F. (1974) Proceedings of the 1973 DoD Laser Effects/Hardening Conference (U), Vol. V, Laser supported absorption waves, Mitre Corp. Rpt M73-115.
7. Edwards, A., Ferriter, N. M., Fleck, J. A., and Winslow, A. M. (1974) A theoretical description of pulsed laser-target interaction in an air environment, published in Proceedings of the 1973 DoD Laser Effects/Hardening conference (U), Vol. V (see ref. 6, p. 115).
8. Stamm, M. R. and Nielsen, P. E. (1974) Nonequilibrium effects in shock- and transport-induced LAW formation, published in Proceedings of the 1973 DoD Laser Effects/Hardening Conference (U), Vol. V (see ref. 6, p. 141).
9. Papa, R. J. (1974) Propagation of High-Power Laser Radiation in Partially Ionized Gases, AFCRL-TR-74-0532.
10. Thomas, P. D. (1973) Laser-Absorption Wave Initiation in Air Over Vaporizing Targets (see ref. 6, p. 69).
11. Klosterman, E. L., Byron, S. R., and Newton, J. F. (1973) Laser Supported Combustion Waves Study Report No. 73-101-3, Mathematical Sciences Northwest, Inc., Seattle, Wash.
12. Walters, C. T. (1972) Review of Experiments at Battelle presented at the Workshop on Laser-Induced Combustion Waves, Seattle, Wash., 5-6 December 1972.

13. Musal, H. M. (1973) Prompt Initiation of Laser-Supported Absorption Waves in Air Via Field-Emission from Target Surfaces (see ref. 8, p. 157.)
14. Walters, C. T. (1973) Experimental Studies of LSD Wave Initiation on Aluminum Targets (see ref. 8, p. 170).
15. Cohen, H. D., Su, F. Y., and Boni, A. A. (1973) A Simple Nonequilibrium Model for a Shock-Heated Monatomic Gas Irradiated by an Intense Laser Beam (see ref. 8, p. 239).
16. Holt, E. H. and Haskell, R. E. (1965) Foundations of Plasma Dynamics, Macmillan.
17. Hora, H. (1969) Phys. Fluids 12:182.
18. Vinogradov, A. V. and Pustovalov, V. V. (1972) Soviet Jour. Quant. Electronics 2:91.
19. Anisimov, S. I. (1967) Soviet Phys. Tech. Phys. 11:945.
20. Stark, P. A. (1970) Introduction to Numerical Methods, Macmillan.
21. Richtmyer, R. D. and Morton, K. W. (1967) Difference Methods for Initial Value Problems, Interscience.
22. Papoular, R. (1972) The initial stages of laser induced gas breakdown, article in Laser Interaction and Related Plasma Phenomena, Vol. 2, Proc. of the Second Workshop held at RPI, Hartford Graduate Center, edited by H. J. Schwarz and H. Hora, Plenum Press.
23. Keldysh, L. V. (1965) Soviet Physics JETP 21:1135.
24. Ramsden, S. A. (1968) Physics of Hot Plasmas, Scottish Universities Summer School, Plenum Press.
25. Myslenkov, V. I. and Raizer, Yu. P. (1972) Soviet Phys. JETP 34:1001.
26. Papa, R. J. (1965) Can. J. Physics 43:38.
27. Papa, R. J. (1968) Can. J. Physics, 46:889.
28. Ginzburg, V. L. (1964) The Propagation of Electromagnetic Waves in Plasmas, Pergamon Press.
29. Lin, S. C. and Teare, J. D. (1962) Avco Research Report 115, Contract No. AF19(604)-7458.
30. Zeldovich, Ya. B. and Raizer, Yu. P. (1966) Physics of Shock Waves and High-Temperature Hydrodynamic Phenomena, Vol. 1, Academic Press.
31. McDaniel, E. W. (1964) Collision Phenomena in Ionized Gases, John Wiley and Sons.
32. Massey, H. S. W., Burhop, E. H. S., and Gilbody, H. B. (1968) Electronic and Ionic Impact Phenomena, Oxford Clarendon Press.
33. Shkarofsky, I. P., Johnston, T. W., and Bachynski, M. P. (1966) The Particle Kinetics of Plasmas, Addison-Wesley.
34. IBM Application Program (1970) System/360 Scientific Subroutine Package, Version III, edition GH20-0205-4.
35. Hildebrand, F. B. (1956) Introduction to Numerical Analysis, McGraw-Hill.